The American Journal of Pathology, Vol. 181, No. 5, November 2012

http://dx.doi.org/10.1016/j.ajpath.2012.08.006

Cell Injury, Repair, Aging, and Apoptosis

Keloid Disease Can Be Inhibited by Antagonizing Excessive mTOR Signaling With a Novel Dual TORC1/2 Inhibitor

Farhatullah Syed,*† David Sherris,‡ Ralf Paus,†§ Shohreh Varmeh,¶ Pier P. Pandolfi,¶ and Ardeshir Bayat*†‖**

From Plastic and Reconstructive Surgery Research, Manchester Institute of Biotechnology, and the Institute of Inflammation and Repair,† University of Manchester, Manchester, United Kingdom; Paloma Pharmaceuticals, Inc.,‡ Boston, Massachusetts; the Department of Dermatology,§ University of Luebeck, Luebeck, Germany; the Beth Israel Deaconess Cancer Center, Department of Medicine and Pathology,¶ Beth Israel Deaconess Medical Center, Harvard Medical School, Boston, Massachusetts; the Department of Plastic and Reconstructive Surgery,‖ and the University of Manchester, Manchester Academic Health Science Centre,** University Hospital South Manchester NHS Foundation Trust, Wythenshawe Hospital, Manchester, United Kingdom*

Keloid disease (KD) is a fibroproliferative lesion of unknown etiopathogenesis that possibly targets the PI3K/Akt/mTOR pathway. We investigated whether PI3K/Akt/mTOR inhibitor, Palomid 529 (P529), which targets both mammalian target of rapamycin complex 1 (mTORC-1) and mTORC-2 signaling, could exert anti-KD effects in a novel KD organ culture assay and in keloid fibroblasts (KF). Treatment of KF with P529 significantly ($P < 0.05$) inhibited cell spreading, attachment, proliferation, migration, and invasive properties at a low concentration (5 ng/mL) and induced substantial KF apoptosis when compared with normal dermal fibroblasts. P529 also inhibited hypoxia-inducible factor-1α expression and completely suppressed Akt, GSK3β, mTOR, eukaryotic initiation factor 4E-binding protein 1, and S6 phosphorylation. P529 significantly ($P < 0.05$) inhibited proliferating cell nuclear antigen and cyclin D and caused considerable apoptosis. Compared with rapamycin and wortmannin, P529 also significantly ($P < 0.05$) reduced keloid-associated phenotypic markers in KF. P529 caused tissue shrinkage, growth arrest, and apoptosis in keloid organ cultures and substantially inhibited angiogenesis. pS6, pAkt-Ser473, and mTOR phosphorylation were also suppressed *in situ*. P529 reduced cellularity and expression of collagen, fibronectin, and α-smooth muscle actin (substantially more than rapamycin). These pre-clinical *in vitro* and *ex vivo* observations are evidence that the mTOR pathway is a promising target for future KD therapy and that the dual PI3K/Akt/mTOR inhibitor P529 deserves systematic exploration as a candidate agent for the future treatment of KD. ***(Am J Pathol 2012, 181: 1642–1658; http://dx.doi.org/10.1016/j.ajpath.2012.08.006)***

The mammalian target of rapamycin (mTOR) is a 289-kDa serine-threonine kinase that regulates cell mobility, survival, proliferation, transcription, and protein synthesis[1–3] and is a negative regulator of autophagy.[4–6] Inhibition of the mTOR pathway has recently become of major interest in the control of tumor growth.[5,7–9] Keloid scars are benign skin lesions that arise from an abnormal wound healing process in genetically susceptible individuals,[10,11] and have a high recurrence rate after surgery.[12] Primary fibroblasts isolated from keloids exhibit some "cancer-like" activities and features,[13–15] and invasive keloid growth has been compared to malignant growth.[15,16] However, keloids are not truly malignant neoplasms because they never metastasize. In KD, there is excessive angiogenesis and inflammatory cell infiltration,[13,17–21] and, therefore, the mTOR pathway may be a plausible target pathway in management of KD.

Supported by personal award from the National Institute for Health Research (A.B.).

Accepted for publication August 1, 2012.

Supplemental material for this article can be found at *http://ajp.amjpathol.org* or at *http://dx.doi.org/10.1016/j.ajpath.2012.08.006*.

Disclosure: D.S. is CEO and president of Paloma Pharmaceuticals, Inc., which donated P529 for this project.

A guest editor acted as editor-in-chief for the manuscript. No person affiliated with the University of Manchester was involved in the final disposition of this article.

Address reprint requests to Ardeshir Bayat, M.B.B.S., Ph.D., Plastic and Reconstructive Surgery Research, Manchester Institute of Biotechnology, University of Manchester, 131 Princess St, Manchester, M1 7ND UK. E-mail: ardeshir.bayat@manchester.ac.uk.

mTOR kinases form two distinct multiprotein complexes: mTORC1 and mTORC2. mTORC1 consists of regulatory associated protein of mTOR (Raptor), mLST8 (also known as G-protein β-subunit–like protein, a yeast homolog of LST8), and PRAS40 (proline-rich Akt substrate of 40 kDa). mTORC2 contains mTOR and mLST8, but instead of Raptor, mTORC2 contains rapamycin-insensitive companion of mTOR (Rictor) and mammalian stress-activated protein kinase-interacting protein-1 (mSin1).[6,22–24]

One of the well-studied allosteric inhibitors of mTOR is rapamycin.[23,25] mTORC1, the molecular target of rapamycin, phosphorylates downstream proteins S6K (p70S6 kinase) and 4E-BP1 (eukaryotic initiation factor 4E-binding protein 1), both involved in translation. However, inhibition of mTORC1 alone by rapalogs could lead to enhanced activation of the PI3K axis because of the mTOR-S6K-IRS1 negative feedback loop.[26,27] mTORC2 phosphorylates Akt on Ser473, increasing its enzyme activity up to 10-fold.[28–30] Activated Akt regulates cell growth, proliferation, cell cycle, apoptosis, and glucose metabolism.[28–30] Considering the importance of Akt signaling and the critical role of mTORC2 in Akt activation, mTORC2, has become an attractive drug target for many cancers.

Aside from its association with cancer,[5,30] dysregulation of the mTOR pathway has been linked to several fibrotic diseases including KD.[31–34] KD is a dermal fibroproliferative disorder characterized by excess scar tissue deposited at the site of cutaneous injury.[19,34–36] There is excessive deposition of extracellular matrix (ECM) components such as collagen, fibronectin, and α-smooth muscle actin (α-SMA).[19,31] Keloid fibroblasts (KF) possess bioenergetic properties that resemble those of cancerous cells[13] and, like these cells, exhibit overexpression of cytokines and growth factors including excessive expression of vascular endothelial growth factor.[17,37] The scar tissue infiltrates the surrounding healthy tissue, and the recurrence rate after excision is as great as 80%.[38] Therefore, KD is considered an aggressive quasi-neoplastic skin lesion of unknown origin.[13,39–41] Many methods are available for treatment of KD; however, they often fail to produce a satisfactory outcome.[42–44]

The mTOR pathway regulates collagen I expression via a PI3K-independent[45] pathway in human dermal fibroblasts, and the PI3K/Akt/mTOR pathway is responsible for overproduction of collagen and ECM in KD.[31,32,46,47] Of note, rapamycin also inhibits ECM deposition.[31,45] Hence, the PI3K/Akt/mTOR pathway is a potential therapeutic target for the future management of KD.[31–35,48] The challenge, therefore, is to generate convincing pre-clinical evidence in support of this novel KD treatment strategy, ideally using the best pre-clinical KD research assay that is currently available, ie, KD organ culture (OC),[21] and to identify well-tolerated mTOR inhibitors that effectively antagonize KD growth and ECM deposition *in vitro* and *in situ*.

To meet this challenge, we hypothesized that dual mTORC-1 and mTORC-2 inhibition would provide superior inhibition of Akt signaling and angiogenesis and would produce a greater effect on KF and KD vasculature than does inhibition of mTORC-1 alone. Unlike rapamycin, which inhibits only mTORC-1,[23,26,49] the novel PI3K/Akt/mTOR inhibitor Palomid 529 (P529) inhibits both mTORC-1 and mTORC-2 signaling.[24,27,50–53]

Therefore, we investigated the following areas in the present study: whether the baseline cellular levels of mTOR and p70S6K and their activated forms differ between primary KF and normal dermal fibroblasts (NF) isolated from extralesional and normal healthy skin; whether P529 antagonizes KD growth and ECM deposition *in vitro* and *in situ* in a manner that renders this novel dual mTORC1/2 inhibitor an ideal candidate for clinical testing in the future management of KD; and whether and how P529 differs in this respect from standard PI3K/Akt/mTOR inhibitors (rapamycin and wortmannin).

Materials and Methods

Patient Selection and Recruitment

Keloid tissue was harvested during excisional surgery in patients confirmed to have clinical and pathologic evidence of KD as described previously[19,36,54] (Figure 1A). Included in the study were 31 patients (16 men and 15 women; age range, 17–74 years) with KF, including 8 with extralesional fibroblasts (normal skin adjacent to a keloid lesion), and 11 patients with NF (4 men and 7 women; age range, 23–65 years). Of 31 keloid tissue samples, 11 were used for *ex vivo* KD OC study (see Supplemental Figure S1 at *http://ajp.amjpathol.org*). Tissue samples were selected carefully from patients with no previous treatment history. In most of the *in vitro* experiments, samples were matched for sex and age (patient demographic data are given in Supplemental Tables S1 and S2 at *http://ajp.amjpathol.org*). Keloid samples were obtained from individuals of different races/ethnicities, all of whom had given approval (obtained from the local hospital, university, and regional NHS Ethics Committee) before the surgical procedure.

Establishment of KF and NF Cell Cultures

Primary fibroblast cell cultures were established as described previously.[19,54] In brief, tissue was washed in PBS (PAA Laboratories, Ltd., Yeovil, Somerset, UK) and incubated in 10 mg/mL dispase II (Roche Diagnostics, Ltd., Burgess Hill, West Sussex, UK) for 3 hours at 37°C, and epidermis and fat were removed. Next, the dermis was minced and incubated in 10 mg/mL collagenase A (Roche Diagnostics). The tissue/cell suspension was passed through a 100-μm filter (cell strainer; BD Biosciences, Oxford, UK) to remove any remaining tissue residuals. Cells were then washed once with PBS and plated in T25 CellBind flasks (Nunc, Life Technologies Ltd., Wiesbaden, Germany) as passage 0 (p0) cells. Cells were maintained in DMEM (Dulbecco's modified Eagle's medium). Passage 1 (p1) to passage 4 (p4) cell cultures were used in the present study.[19,54]

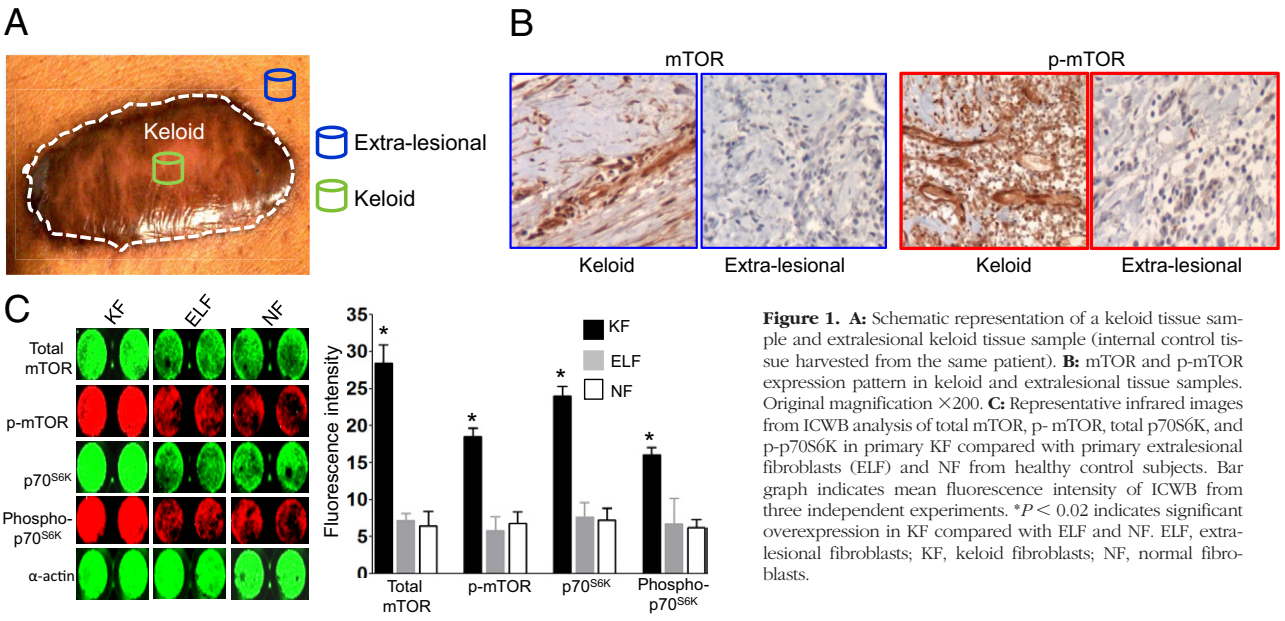

Figure 1. **A:** Schematic representation of a keloid tissue sample and extralesional keloid tissue sample (internal control tissue harvested from the same patient). **B:** mTOR and p-mTOR expression pattern in keloid and extralesional tissue samples. Original magnification ×200. **C:** Representative infrared images from ICWB analysis of total mTOR, p- mTOR, total p70S6K, and p-p70S6K in primary KF compared with primary extralesional fibroblasts (ELF) and NF from healthy control subjects. Bar graph indicates mean fluorescence intensity of ICWB from three independent experiments. $*P < 0.02$ indicates significant overexpression in KF compared with ELF and NF. ELF, extralesional fibroblasts; KF, keloid fibroblasts; NF, normal fibroblasts.

P529, Rapamycin, Wortmannin, and Camptothecin Regimen

P529 was provided by Paloma Pharmaceuticals, Inc. (Boston, Massachusetts). Rapamycin and wortmannin were purchased from Merck Chemicals, Ltd. (Beeston, Nottingham, UK) to assess and compare the effect of P529. The concentration of rapamycin was determined on the basis of similar studies of primary fibroblasts.[31] The following concentrations were compared: P529 (5, 10, 20, and 40 ng/mL), rapamycin (50 and 100 ng/mL), and wortmannin (5 and 10 ng/mL). Camptothecin (Sigma-Aldrich Corp., St. Louis, MO) (250 ng/mL) was used as a positive control for real-time cell analysis (RTCA), cytotoxicity assay via detection of lactate dehydrogenase (LDH), viability/metabolic activity assay via water-soluble tetrazolium salts-1 (WST-1), and apoptotic assay (see Supplemental Figure S1 at *http://ajp.amjpathol.org*).

Label-Free RTCA

To determine the effect of various drug concentrations on KF compared with NF *in vitro*, label-free RTCA was used, as described previously.[19,55,56]

Cytotoxicity (LDH) and Cell Viability/Metabolic Activity (WST-1) Assay

LDH and WST-1 (Roche Diagnostics) assays were performed according to the manufacturer's instructions after various drug therapies, as indicated above.

High Throughput In-Cell Western Blotting and Quantification

Primary KF and NF were subjected to various concentrations of mTOR drugs, as indicated above, for 24 hours at 37°C in 5% CO_2. Then, In-Cell Western Blotting (ICWB) was performed using the similar protocol as described previously.[19,54,55] In brief, KF and NF were grown to 80% to 85% confluence in T75 flasks. Before inoculating the cells in 96-well plates, the cells were starved in 0.2% serum DMEM for 24 hours. Cells were trypsinized and counted using FACS (fluorescence-activated cell sorting), and 10,000 cells were inoculated in each well of the 96-well plates (Dow Corning, Ltd., Barry, Vale of Glamorgan, UK) in triplicate and grown in DMEM for up to 7 to 8 hours at 37°C in 5% CO_2. The cells were then treated for 24 hours using various drugs. Subsequent to this, the cells were fixed in 4% formaldehyde for 30 minutes at room temperature. The wells were washed three times with PBS (200 μL/well), permeabilized with PBS/0.1% Triton X-100 (150 μL/well, three times for 5 minutes each), and blocked in Odyssey blocking buffer (LI-COR Biosciences UK, Ltd., Cambridge, UK) (200 μL/well) for 2 hours at room temperature. The 96-well plates were then incubated using various primary antibodies (Table 1) overnight at 4°C (50 μL/well). They were subsequently washed three times with PBS/0.1% Tween-20 (150 μL/well). Secondary antibody (1:500) in PBS/0.5% Tween-20 was then added (50 μL/well) (Table 2). The plates were then incubated for 1 hour at room temperature, and the wells were washed with PBS/0.1% Tween-20 three times. The plates were covered with aluminum foil and imaged on an Odyssey infrared scanner (LI-COR Biosciences) using microplate 2 setting with sensitivity of 7 in the 800-nm wavelength channel. Data were retrieved using Odyssey software, which were then exported and analyzed using Excel software (Microsoft Corp., Redmond, WA). β-Actin was used as loading control.

Measurement of Early Apoptosis via Annexin V Staining Followed by FACS

Primary KF and NF were treated using various concentrations of P529, rapamycin, and wortmannin, as de-

Table 1. Primary Antibodies Used in the Present Study

Antibody	Species raised	Isotype	Clone	In-cell Western dilution	IHC-dilution	Product code	Source
S6 ribosomal protein	Mouse monoclonal	IgG1	54D2	1:1000	1:100	2317	CST
pS6 ribosomal protein (Ser235/236)	Rabbit monoclonal	IgG	91B2	1:1000	1:75	4857	CST
p70S6K	Rabbit monoclonal	IgG	NA	1:500	NA	9202	CST
p-p70S6K	Rabbit monoclonal	IgG	NA	1:500	NA	9204	CST
AKT	Rabbit	NA	NA	1:1000	1:200	9272	CST
p-AKT (Thr308)	Rabbit monoclonal	IgG	244F9	1:1000	NA	4056	CST
p-AKT (Ser473)	Rabbit monoclonal	IgG	D9E	1:1000	1:50	4060	CST
mTOR	Rabbit	NA	NA	1:1000	1:100	2972	CST
p-mTOR (Ser2448)	Rabbit	NA	NA	1:1000	1:100	2971	CST
GSK-3-α/β	Rabbit monoclonal	IgG	D75D3	1:1000	NA	5676	CST
p-GSK-3-α/β (Ser9)	Rabbit monoclonal	IgG	5B3	1:1000	1:400	9323	CST
p38 MAP kinase	Rabbit	NA	NA	1:1000	1:50	9212	CST
p-p38 MAP kinase (Thr180/Tyr182)	Rabbit	NA	NA	1:1000	NA	9211	CST
PCNA	Mouse monoclonal	IgG2a	PC10	1:2000	1:4000	2586	CST
Cyclin D1	Rabbit monoclonal	IgG	92G2	1:1000	1:25	2978	CST
Anti-HIF-1α	Mouse monoclonal	IgG1	ESEE122	1:500	NA	Ab8366	Abcam
Collagen I	Mouse monoclonal	IgG1	COL-1	1:500	1:200	Ab6308	Abcam
CD34	Mouse monoclonal	IgG1	581	NA	1:100	Ab45524	Abcam
CD31	Mouse monoclonal	IgG1	1A10	NA	1:50	ncl-cd31-1a10	Leica
α-SMA	Mouse monoclonal	IgG2a	1A4	1:500	1:250	A5691	Sigma-Aldrich
Fibronectin	Rabbit polyclonal	IgG	NA	1:500	1:250	ab2413	Abcam
β-Actin	Mouse monoclonal	IgG1	NA	1:1000	NA	Ab8226	Abcam

Abcam PLC, Cambridge, UK; CST, Cell Signaling Technology, Inc., Danvers, MA; Leica Microsystems (UK), Ltd., Milton Keynes, Buckinghamshire, UK; NA, not available or not applicable; Sigma-Aldrich Corp., St. Louis, MO.

scribed above. Apoptosis was detected using an annexin V–FITC (fluorescein isothiocyanate)–labeled apoptosis detection kit (Abcam PLC, Cambridge, UK) as described previously.[55]

In Vitro *Two-Dimensional Migration Assay*

Each well of a 96-well Oris plate (Oris migration assay kit; Cambridge Bioscience, Ltd., Cambridge, UK) was coated with 9 μg/mL collagen (BD Biosciences) and incubated for 30 to 45 minutes at 37°C in 5% CO_2. After incubation, wells were rinsed with 1X PBS once, and Oris cell seeding stoppers were inserted according to the manufacturer's instructions. Serum-starved KF and NF were prelabeled with PKH26 (Sigma-Aldrich) according to the manufacturer's instructions, and 2.5×10^4 cells per well were seeded in triplicate. For each treatment, one well without a cell-seeding stopper served as the positive control. The plate was then incubated overnight at 37°C in 5%CO_2. The next day, the cell-seeding stoppers were removed from the test wells, and cells were washed once with PBS 1X (PAA Laboratories). Then 100 μL fresh medium was added with or without various drugs, and the cells were allowed to migrate for ~30 hours in the migration zone created by cell-seeding stoppers. After completion of the experiment, micrographs were captured using an inverted IX71 microscope (Olympus Corp., Tokyo, Japan) at ×4 magnification. Migrated cells in the migration zone were counted from four independent experiments, and the mean number of migrated cells was plotted on the graphs.

In Vitro *Three-Dimensional Invasion Assay*

Inhibition of the invasive capacity of primary KF was tested using an *in vitro* three-dimensional (3D) invasion assay (Oris invasion and detection assay kit; Cambridge Bioscience) as described previously.[19] In brief, 96-well plates were coated with basement membrane extract (BME) per the manufacturer's instructions. After BME coating, Oris cell-seeding stoppers were inserted in each well. Serum-starved cells, 2.5×10^4 cells/well, were

Table 2. Secondary Antibodies Used in the Present Study

Antibody	Species raised	Isotype	Active against	Dilution	Product code	Source
Goat anti-mouse-Alexa Fluor-488	Goat	IgG, IgM (H+L)	Mouse	1:250	A10680	Invitrogen
Donkey anti-mouse IRDye 800CW	Donkey	IgG	Mouse	1:800	926–32212	LI-COR
Donkey anti-rabbit IRDye 800CW	Donkey	IgG	Rabbit	1:800	926–32213	LI-COR
Donkey anti-mouse IRDye 680CW	Donkey	IgG	Mouse	1:800	926–32222	LI-COR
Donkey anti-rabbit IRDye 680CW	Donkey	IgG	Rabbit	1:800	926–32223	LI-COR
Donkey anti-goat IRDye 680CW	Donkey	IgG	Goat	1:800	926–32224	LI-COR

Invitrogen Corp., Carlsbad, CA; LI-COR Biosciences UK, Ltd., Cambridge, UK.

seeded. At 8 to 12 hours after cell attachment, the stoppers were removed, the cells were washed once with 1X PBS, and 40 μL BME was added on top of the cells. The plates were reincubated at 37°C in 5% CO2 for 45 to 60 minutes to enable polymerization of BME. After BME polymerization, various mTOR drug treatments were given for ~48 hours, and the cells were allowed to invade (in the presence of mTOR drugs) the 2-mm invasion zone created by cell-seeding stoppers. After completion of the experiment, cells were stained with calcein AM. Micrographs were obtained using an inverted IX71 microscope (Olympus) at ×4 magnification. Invaded cells in the invasion zone were counted from four independent experiments, and the mean number of invaded cells were plotted on graphs.

Actin Reorganization

Serum-starved, low-density (1.5×10^4 cells/well), primary KF (passages p1 to p4) were grown on glass coverslips in 24-well plates, were pre-treated with or without P529, rapamycin, and wortmannin for ~8 hours, then stimulated with or without 10 ng/mL insulin-like growth factor-1 (IGF-1) (R&D Systems Europe, Ltd., Abingdon, Oxfordshire, UK) for ~3.5 hours. Cells were then fixed in 4% paraformaldehyde buffered solution for 20 minutes at 4°C and permeabilized with 0.1% Triton X-100 in 1× PBS (PAA Laboratories) for 15 minutes. Cells were stained with 1 mg/mL TRITC-conjugated phalloidin (Sigma-Aldrich) for 30 minutes at room temperature. Actin filaments (F-actin) were visualized and photographed using a BX53 digital microscope (Olympus). The percentage of cells with lamellipodia formation was determined by randomly counting at least 250 cells under the fluorescence microscope at ×600 magnification.

Ex Vivo *Keloid OC Model*

For the serum-free long-term OC of keloid tissue, a recently developed KD OC system was used.[36] In brief, 4-mm punch biopsy fragments were prepared from keloid tissue. These were embedded in rat tail collagen gel matrix at the air-liquid interface. Serum-free William's E medium, supplemented with 10 μg/mL insulin, 10 ng/mL hydrocortisone, 2 mmol/L L-glutamine, 100 IU/mL penicillin, and 10 μg/mL streptomycin,[57] was used to maintain keloid OC up to 4 weeks (for methodologic details, see Bagabir et al[36]).

Keloid OC Volume Shrinkage and Epidermal Shrinkage

Keloid OC shrinkage, epidermal shrinkage, and cellularity after treatment with various mTOR drugs were assessed as described previously.[36]

Histochemistry

Tissue specimens were fixed in formaldehyde, embedded in paraffin blocks, and sectioned to 4- to 5-μm thickness. Paraffinized tissue sections (4 to 5 μm) collected at various times (day 0, day 3, week 1, week 2, and week 4) were deparaffinized and stained using standard H&E (Surgipath; Leica Microsystems (UK), Ltd., Milton Keynes, Buckinghamshire, UK). Micrographs were obtained using an upright fluorescence microscope (BX51; Olympus).[19,36,54]

Immunohistology

Tissues were immersed in freshly prepared 4% paraformaldehyde in 0.02 mol/L phosphate buffer (pH 7.4) overnight at 4°C, washed in 1 × PBS, and embedded in paraffin. For immunostaining, 4- to 5-μm tissue sections were hydrated and incubated in 3% H_2O_2 in methanol for 20 minutes, washed in water, and boiled in 1 mmol/L EDTA (pH 8.0) for 15 to 20 minutes. Sections were blocked with 3% to 6% normal goat serum (Vector Laboratories, Ltd., Orton Southgate, Peterborough, UK) and incubated with various primary antibodies (Table 1) at specific dilutions overnight at 4°C. After two washes with 1× Tris-buffered saline solution, tissue sections were incubated with respective secondary antibodies (Table 2) for 30 to 45 minutes at room temperature and detected using an avidin-biotin complex method kit (Vector Laboratories).[19,36]

Apoptosis Detection in Situ

To evaluate apoptosis caused by the various concentrations of drugs, double immunofluorescence was used. Terminal dUTP nick-end labeling [Dead-End TUNEL assay; Promega (UK), Ltd., Southampton, Hampshire, UK) was used as a marker for apoptosis, and DAPI was used to localize the DNA as described previously.[36] The micrographs were obtained using an upright fluorescence microscope (BX51; Olympus) at ×200 magnification. The mean number of apoptotic cells was quantified in five random fields from each stained tissue section.

OC Fluorescence-Associated Immunohistochemistry

Cell-specific antigen (CD34 expression) was localized on 4- to 5-μm paraffin sections using a similar technique as described previously.[36]

Statistical Analysis

Each experiment was performed independently at least three or four times. Data are given as mean ± SEM. Statistical evaluation of the continuous data was performed using one-way analysis of variance, followed by Dunnett's *t*-test for between-group comparisons. Statistical analyses were performed using commercially available software (SPSS version 13.0; SPSS, Inc., Chicago, IL). $P < 0.05$ was considered statistically significant.

Results

Elevated Levels of Total and Phosphorylated Forms of mTOR and p70^{S6K} in KF

mTOR regulates metabolic processes and translation rates in response to intracellular ATP levels, as well as extracellular signals by phosphorylating two major translational components: ribosomal p70KDa S6 kinase (p70^{S6K}) and eIF4E.[58,59] mTOR, p70^{S6K}, and their phosphorylated forms are up-regulated in KF compared with NF.[31] Hence, we initially investigated whether there was overexpression of mTOR, p70^{S6K}, and their phosphorylated forms in the keloid samples.

Immunoperoxidase staining for total and phosphorylated forms of mTOR showed high expression in KD tissue (n = 7) compared with extralesional tissue sections (n = 5) (Figure 1B). ICWB analysis and mean total immunoreactivity (fluorescence intensity) also exhibited significant ($P < 0.02$) up-regulation of mTOR, p-mTOR, p70^{S6K}, and p-p70^{S6K} in KF (n = 12) compared with fibroblasts isolated from extralesional sites (n = 8) and normal skin (n = 5) (Figure 1C). There was also noticeable overexpression of pS6, one of the downstream targets of the mTOR signaling pathway, in KD compared with normal skin tissue (see Supplemental Figure S2 at *http://ajp.amjpathol.org*). However, there was no statistically significant difference in the expression of mTOR, p70^{S6K}, and their phosphorylated forms between primary extralesional fibroblasts and NF (Figure 1C). These analyses demonstrate that mTOR is highly active in KD lesions compared with extralesional and normal skin.

Dose-Dependent Effect of P529 on PI3K/Akt/mTOR signaling in KF

We next investigated the efficacy of P529 on intracellular PI3K/Akt/mTOR signaling of primary human KF (n = 10) and NF (n = 6). This was compared with rapamycin, the reference mTOR inhibitor, and wortmannin, a specific inhibitor of PI3K signaling, using ICWB. Results showed a statistically significant ($P < 0.02$) concentration-dependent decrease in pAkt-S473 in primary KF at 24 hours of treatment with both P529 and wortmannin, whereas total Akt levels were unaffected by both compounds. mTORC1 downstream substrates, 4E-PB, and S6 ribosomal protein were also efficiently ($P < 0.02$) dephosphorylated by both compounds. Both P529 and wortmannin inhibited neither phosphorylated mitogen-activated protein kinase nor pAkt-T308 as potently as pAkt-S473. Furthermore, P529 successfully reduced ($P < 0.02$) phosphorylation of p-GSK3β, a critical downstream element of the PI3kinase/Akt cell survival pathway, and HIF1-α ($P < 0.02$). As expected, rapamycin (100 ng/mL) reduced pAkt-S473 at very low levels, compared with both P529 and wortmannin (5 ng/mL), at a higher concentration of 100 ng/mL (Figure 2, A and B). P529 did not cause any significant

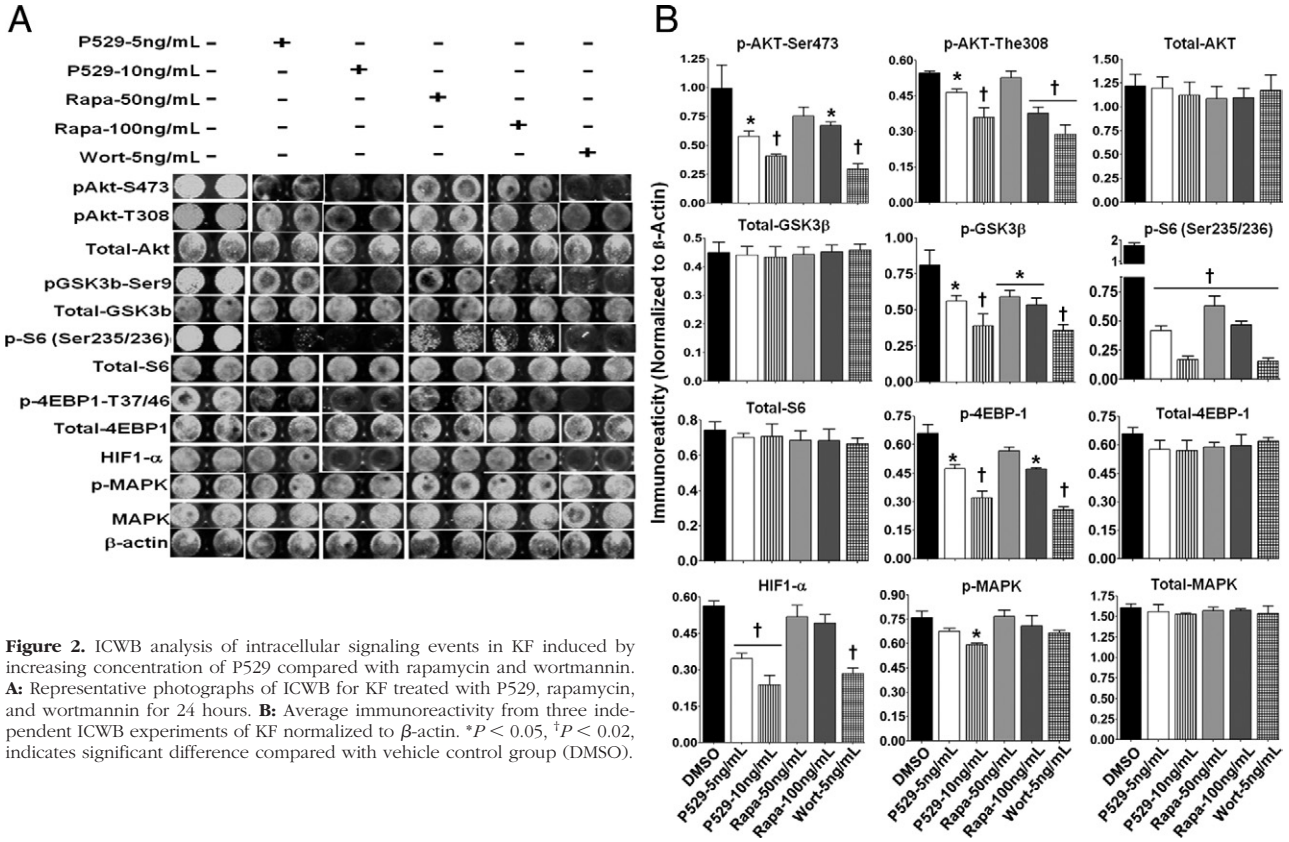

Figure 2. ICWB analysis of intracellular signaling events in KF induced by increasing concentration of P529 compared with rapamycin and wortmannin. **A:** Representative photographs of ICWB for KF treated with P529, rapamycin, and wortmannin for 24 hours. **B:** Average immunoreactivity from three independent ICWB experiments of KF normalized to β-actin. $^{*}P < 0.05$, $^{\dagger}P < 0.02$, indicates significant difference compared with vehicle control group (DMSO).

inhibition of PI3K/Akt/mTOR signaling in NF at a low concentration (5 ng/mL) as compared with rapamycin and wortmannin (see Supplemental Figure S3 at *http://ajp.amjpathol.org*). Considered together, these results demonstrate that, compared with rapamycin, P529 is a specific and highly potent inhibitor of Akt/mTOR in primary human KF.

Dose-Dependent Inhibition of p-mTOR in KF

Subsequently, we compared the inhibition potency of P529 on p-mTOR with rapamycin and wortmannin. In ICWB, all three compounds showed significantly ($P < 0.02$) reduced p-mTOR levels (Figure 3, A and B). However, rapamycin (100 ng/mL) was less effective in reducing p-mTOR than were P529 and wortmannin (5 ng/mL). Hence, at low concentrations, P529 is a highly potent p-mTOR inhibitor in KF ($n = 8$). Unlike rapamycin and wortmannin, P529 did not have any inhibitory effect on p-mTOR in NF ($n = 5$) (see Supplemental Figure S4 at *http://ajp.amjpathol.org*) compared with KF, which suggests that P529 has a greater p-mTOR inhibitory effect on KF.

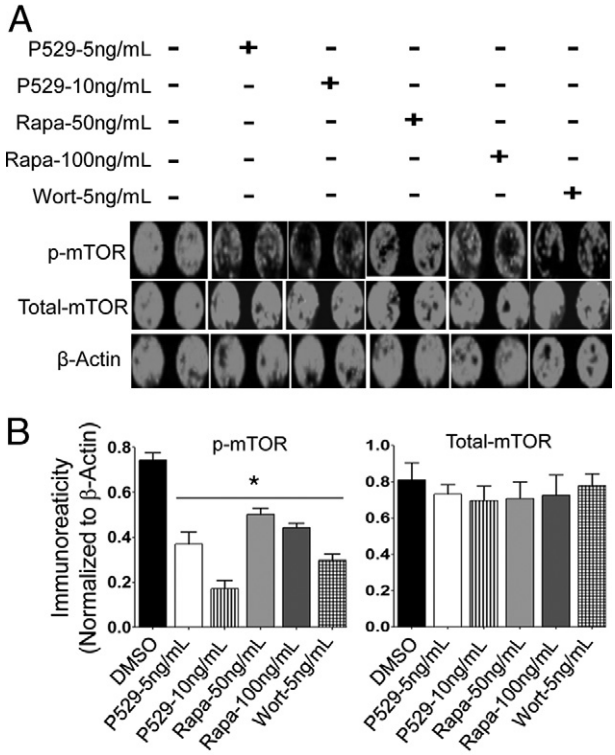

Figure 3. Expression pattern of total and p-mTOR in KF at 24 hours after treatment with P529, rapamycin, and wortmannin. **A:** In-Cell Western Blot was performed to assess the immunoreactivity of mTOR and p-mTOR after various drug treatments. Representative output infrared images of treated and untreated fibroblasts, stained for protein expression (visible in red) are shown. **B:** Bar graphs represent the quantification of mean protein expression with various treatments from three independent experiments after normalization to loading control β-actin. $^*P < 0.05$, significant difference in the treated group vs the vehicle (DMSO) control group.

Dose-Dependent Inhibition of Cell Spreading, Attachment, and Cell Proliferation in KF

We investigated whether P529 has any substantial inhibitory effect at the cellular level on KF and NF activity. We used a label-free RTCA system. RTCA results showed that primary KF ($n = 10$) and NF ($n = 5$) had cell indices of ~3.8 to 4.2 and ~3.0 to 3.7, respectively, at 24 hours of cell growth in the absence of any test compounds. This confirmed that fibroblasts obtained in KD (Figure 4, A and B) were significantly ($P < 0.05$) more aggressive in terms of cell spreading, attachment, and proliferation[13,17,32,60,61] compared with NF (Figure 4B; and see Supplemental Figure S5 at *http://ajp.amjpathol.org*).

By using the RTCA assay, we also demonstrated that P529, rapamycin, and wortmannin inhibited cell spreading, attachment, and proliferation in primary KF in a dose- and time-dependent manner. Compared with rapamycin and wortmannin, P529 was highly effective even at very low concentrations (5 ng/mL). A similar dose- and time-dependent inhibition was also observed in NF, but with slightly less efficacy than in KF. However, compared with rapamycin and wortmannin, P529 was more efficient in inhibiting both primary KF and NF (Figure 4B).

Consequently, we investigated whether P529 had a sustained effect on KF and NF after drug retrieval. In both cell types, when P529 was retrieved, the cells were not able to recover within 30 hours; rather, the average cell index was further reduced, which suggests that the drug effect was sustained in this group compared with groups treated with rapamycin and wortmannin (Figure 4B). These results suggest that P529 decreased KF and NF activity more efficiently than did rapamycin and wortmannin.

Increased Dose-Dependent Cytotoxicity and Cell Viability/Metabolic Activity in KF

To better understand the inhibitory effect of KF and NF observed in the RTCA assay, we assessed the efficacy of P529 on cytotoxicity using an LDH assay, and cell viability/metabolic activity using a WST-1 assay.

Both membrane disturbance (cytotoxicity) and mitochondrial activity (viability/metabolic activity) were studied using a range of concentrations of P529 (5, 10, 20, and 40 ng/mL). All three compounds (P529, rapamycin, and wortmannin) significantly ($P < 0.05$) increased cytotoxicity at various concentrations in primary human KF ($n = 10$) and NF ($n = 6$). However, the P529-treated group exhibited higher cytotoxicity than did the groups treated with rapamycin or wortmannin in KF compared with NF (see Supplemental Figure S6A at *http://ajp.amjpathol.org*). When drug treatments were stopped, P529 sustained cytotoxicity significantly ($P < 0.05$) for up to 30 hours compared with the groups treated with rapamycin or wortmannin. P529 demonstrated significant toxicity in KF and NF; however, the effect was reversible within 24 hours of drug removal in NF but not in KF, and much higher dosages were required for the growth-inhibitory

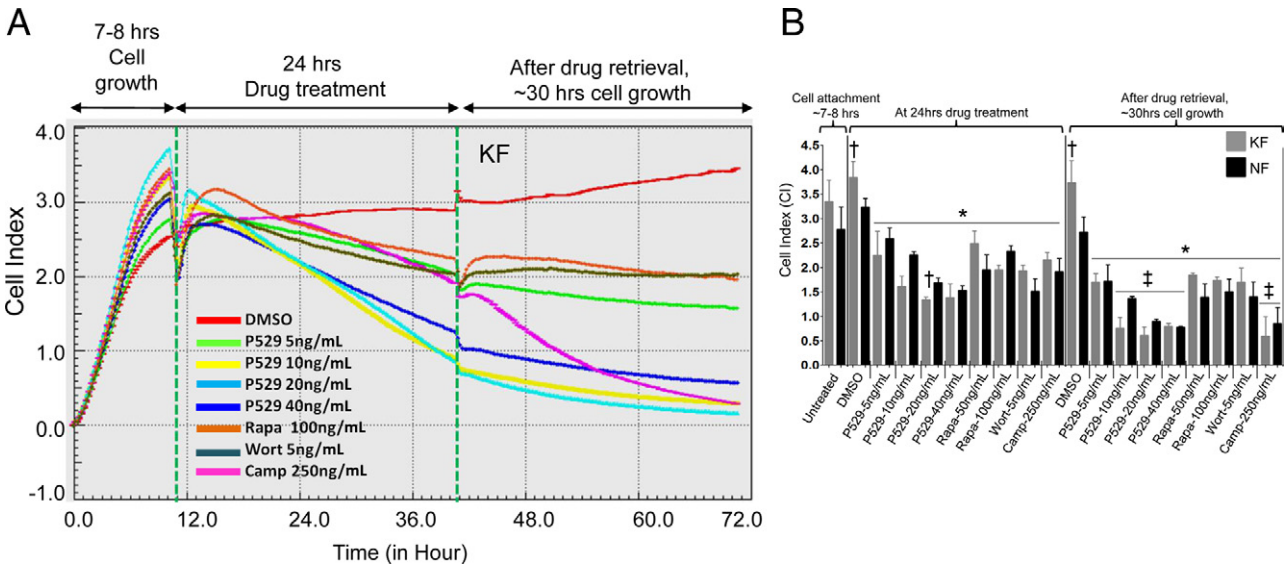

Figure 4. Role of mTOR inhibitors on keloid cell behavior using dynamic and real-time monitoring of cell adhesion, spreading, and proliferation on microelectronic sensor arrays. **A:** Effect of P529, rapamycin, and wortmannin on KF using real-time cell analysis. **B:** Quantitative analysis of RTCA cell index of KF and NF. Representative data from five independent experiments performed in triplicate are shown. $^{*}P < 0.05$, $^{\dagger}P < 0.02$, significant difference vs DMSO control group. $^{\ddagger}P < 0.05$, significant difference in growth of KF versus NF.

effects of P529 in NF compared with KF (see Supplemental Figure S6B at *http://ajp.amjpathol.org*).

WST-1 analysis demonstrated a significant ($P < 0.05$) increase in viability/metabolic activity of primary KF compared with NF. These results were in agreement with those of RTCA. P529 and wortmannin were significantly ($P < 0.05$) more effective in reducing cell viability/metabolic activity in a dose-dependent manner compared with the dimethyl sulfoxide (DMSO) control group (see Supplemental Figure S6C at *http://ajp.amjpathol.org*). However, rapamycin also reduced the viability/metabolic activity of KF at much higher concentrations. Compared with the groups treated with rapamycin, KF in the groups treated with P529 or wortmannin sustained cell viability/metabolic activity inhibition up to 24 to 30 hours after discontinuation of the drug (see Supplemental Figure S6D at *http://ajp.amjpathol.org*). P529 was highly selective and effective in KF and less effective in NF, compared with both rapamycin and wortmannin. From these results, it was concluded that P529 caused severe toxicity and substantially inhibited viability/metabolic activity.

Inhibition of KF Proliferation by Down-Regulation of Cell Cycle

P529 greatly reduced KF and NF proliferation. To further investigate these findings, expression of the cell cycle proteins PCNA and cyclin D, were evaluated at the protein level using ICWB. Significant ($P < 0.02$) concentration-dependent down-regulation of PCNA and cyclin D was detected in fibroblasts treated with both P529 and Wortmannin compared with DMSO. However, at a higher concentration (100 ng/mL), the rapamycin-treated group also exhibited a similar level of significant ($P < 0.02$) reduction in PCNA and cyclin D expression compared with the DMSO control group in both KF ($n = 8$) (Figure 5, A and B) and NF ($n = 5$) (see Supplemental Figure S7 at *http://ajp.amjpathol.org*). Considered together, these results show that P529 significantly inhibits primary KF activity, at least in part by inhibiting PCNA and cyclin D at the molecular level.

Dose-Dependent Induction of Apoptosis in KF

On the basis of these results, we hypothesized that P529 might achieve its inhibitory effect on cell spreading, attachment, and proliferation via apoptosis or cellular necrosis. This hypothesis was assessed via dual-labeled FACS analysis using annexin V and propidium iodide labeling (annexin V detects early apoptosis and propidium iodide identifies cell death and necrosis).[55] P529, rapamycin, and wortmannin all significantly ($P < 0.05$) and dose dependently increased the percentage of cells positive for annexin V and propidium iodide, compared with control. Compared with NF ($n = 4$), P529 caused more apoptosis in KF ($n = 8$) (Figure 6, A and B; and see Supplemental Figure S8 at *http://ajp.amjpathol.org*). Therefore, P529 strongly promotes apoptosis and necrosis in human KF.

Inhibition of Migration and Invasion Properties of KF

These inhibitory properties of P529 were further probed under 2D and 3D conditions, using a novel *in vitro* migration assay. Treatment with P529, rapamycin, and wortmannin significantly ($P < 0.05$) reduced the migration properties of KF ($n = 6$) in 2D migration compared with the control DMSO-treated group in a concentration-dependent manner. As expected, P529 was more potent in inhibiting migration properties of KF than was rapamycin,

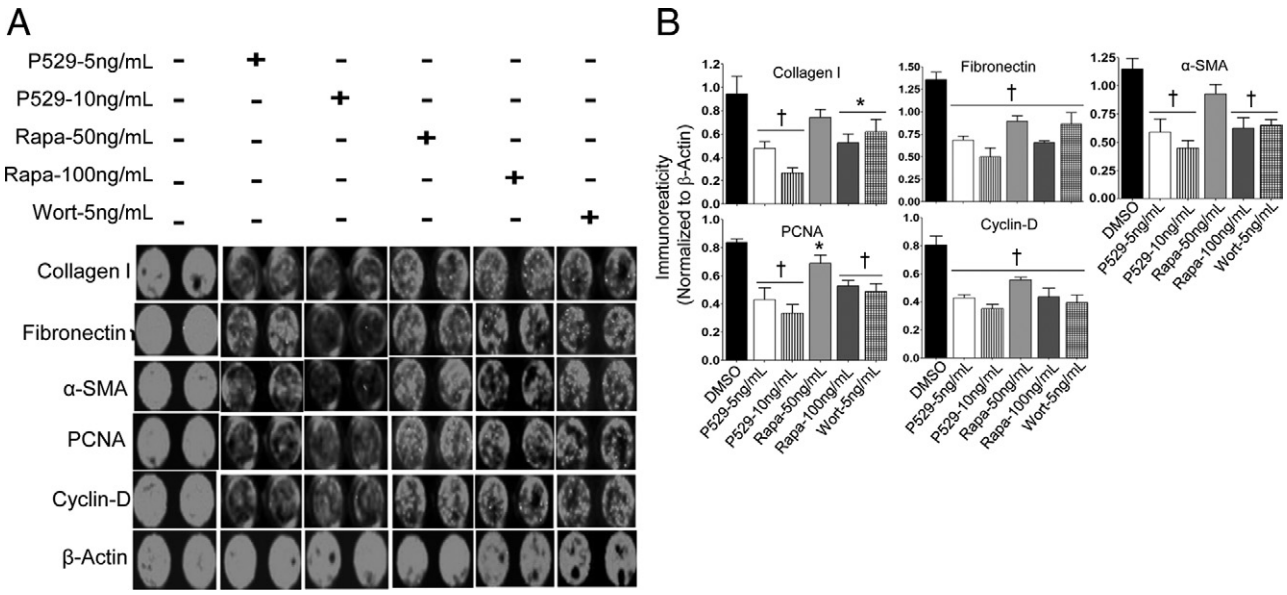

Figure 5. Inhibition of keloid-associated fibrotic markers and cell cycle–regulated genes by P529. **A:** In-Cell Western Blotting of expression of ECM proteins, PCNA, and cyclin D 24 at hours after treatment of KF with various drugs. **B:** Mean immunoreactivity values of KF from three independent experiment of In-Cell Western Blotting plotted on the graphs after normalizing to β-actin. $^{*}P < 0.05$, $^{\dagger}P < 0.02$, significant difference in treated group vs DMSO control group.

even at very low concentrations (Figure 7, A and B). Like other cancer cells, KF have invasive properties.[13,54] As anticipated, in the 3D invasion model, KF ($n = 8$) was highly invasive. Both P529 and wortmannin significantly ($P < 0.01$) reduced the invasive properties of KF at 48 hours after treatment. In addition, rapamycin also showed significant ($P < 0.05$) inhibition of invasion properties of KF, but with very low efficacy (Figure 7, C and D). Considered together, these results suggest that P529 has a potential anti-migration and anti-invasive property for KF.

Inhibition of IGF-1–Stimulated F-Actin Reorganization in KF

Rapid reorganization of the actin cytoskeleton, a multistep process that includes cell polarization, adhesion, and de-adhesion, is an early event in cell migration and invasion.[62,63] Therefore, we attempted to understand whether the P529-induced inhibition of cell migration and invasion is related to prevention of cell polarization or protrusion. This was assessed using an IGF-1–stimulated F-actin reorganization assay.[64] The results showed that, in response to stimulation with IGF-1 (10 ng/mL), the actin cytoskeleton in KF ($n = 8$) undergoes rapid reorganization. P529, rapamycin, and wortmannin did not alter the pattern of basal F-actin distribution, but reduced IGF-1–stimulated F-actin reorganization at the leading edge and lamellipodia formation in KF, compared with the control group. P529 reduced lamellipodia formation more effectively than did rapamycin and wortmannin (Figure 8, A and B). Considered together, these results suggest that P529 significantly inhibits F-actin reorganization, which could be a potential mechanism for inhibition of cell proliferation, migration, and invasion properties of primary KF.

Dose-Dependent Down-Regulated Expression of Fibrosis-Associated Keloid Markers

KD has been associated with a number of molecular markers, and there is increased expression of several key cytokine and growth factors including vascular endothelial growth factor, transforming growth factor-β, platelet-derived growth factor, and connective tissue growth factor. In addition, there is overexpression of a number of characteristic ECM-associated proteins such as collagen, fibronectin, and α-SMA.[17,31,33,37,61,65] Therefore, using ICWB, we compared the effect of P529, rapamycin, and wortmannin on the expression of KD-associated fibrotic markers at the protein level. This demonstrated that all compounds significantly ($P < 0.04$) and dose-dependently down-regulated collagen I, fibronectin, and α-SMA protein expression (Figure 5, A and B), compared with controls. Again, compared with rapamycin and wortmannin, P529 was more effective at very low concentrations (5 ng/mL) in the inhibition of these ECM proteins, which was evident in KF ($n = 8$) (Figure 5, A and B). Compared with rapamycin and wortmannin, P529 did not show significant inhibition of ECM in NF ($n = 5$) (see Supplemental Figure S7 at *http://ajp.amjpathol.org*). In the present study, down-regulation of collagen and fibronectin by P529 ($P < 0.001$) was highly specific for P529 and strongly significant compared with rapamycin ($P < 0.05$) and wortmannin ($P < 0.01$). Because we normalized the expression levels of collagen and fibronectin to β-actin (internal loading control) in ICWB, our data suggest that this effect was not related to apoptosis or necrosis.

Overall, in the present study we demonstrated that P529 significantly inhibited primary KF at very low concentrations. Rather, a significant effect of P529 was observed in primary NF only at much higher concentrations.

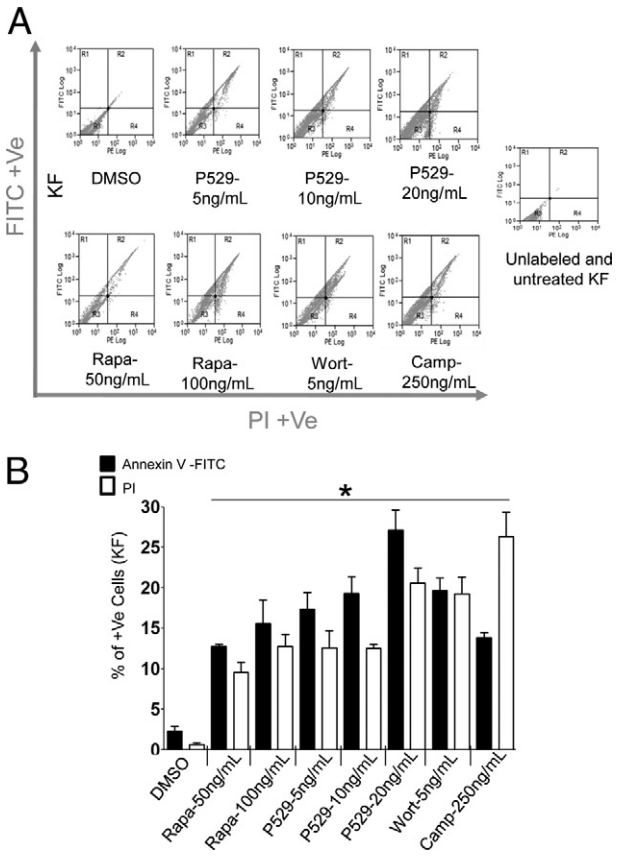

Figure 6. P529 induces apoptosis in KF. Apoptosis was detected with drug treatment using annexin V staining. **A:** Annexin V staining for FACS. After 24 hours of treatment with indicated drug concentrations, the cells were harvested, and FITC-labeled annexin V was added to a final concentration of 2.5 μg/mL. To detect dead cells, propidium iodide (PI) was added at 5 μg/mL concentration. Using flow cytometry, dot plots of annexin V on the *y* axis against PI on the *x* axis were used to differentiate viable cells (negative for both PI and annexin V), apoptotic cells (annexin V–positive cells but excluding PI, with PI therefore negative), and late apoptotic or necrotic cells (double-positive for PI uptake and annexin V staining). Nonstained cells and untreated cells were used as negative controls. **B:** Annexin V– and PI-positive KF after 24 hours of treatment with various drugs as indicated in the bar graphs at different concentrations. Positive cells were counted from three independent experiments and plotted on the graph as mean ± SEM, $*P < 0.05$, significant difference vs DMSO control group.

This suggests the specificity of P529, which acts selectively on cells with active mTOR signaling.

Significant Reduction of Keloid Tissue Volume by P529

To evaluate the therapeutic potential of P529 in the management of KD, 4-mm biopsy samples of KD tissue (n = 11) were subjected to various concentrations of P529 in a serum-free, keloid, long-term OC model.[21] P529 and wortmannin significantly ($P < 0.05$) reduced keloid tissue volume at week 1 (Figure 9A; and see Supplemental Figure S9 at *http://ajp.amjpathol.org*), and weight (Figure 9B) at day 3, compared with the vehicle- and rapamycin-treated groups. However, rapamycin also decreased ($P < 0.05$) the mean volume and weight of the keloid OC after 1 week. These data suggest that P529 induced rapid shrinkage of keloid volume and weight in an *ex vivo* model.

Reduction of Keloid Tissue Epidermal Thickness, Cellularity, Inflammation, and Angiogenesis in Situ

We further delineated the anti-keloid effect of P529 in an *ex vivo* model. Histologic and morphometric analyses of the KD OC (n = 11) showed that the thickness of the epidermis overlying the keloid was significantly (P = 0.01) reduced at week 1 of P529 treatment compared with rapamycin and wortmannin (Figure 9B). Histologic analysis revealed that up to day 3, the overall tissue architecture was well preserved after both wortmannin and rapamycin treatment. Instead, on day 3, thinning of the stratum granulosum and papillary dermis was observed in the P529 treatment group (see Supplemental Figure S10 at *http://ajp.amjpathol.org*). P529 and wortmannin caused severe epidermal damage, with pycnotic nuclei and dislocation of epidermis from dermis, at weeks 1 to 4 after treatment (Figure 10A). In contrast, the rapamycin-treated group exhibited minimal tissue damage from day 3 to week 4. Both P529 and wortmannin suppressed cellularity and inflammation by 20% to 30%, and a noticeable decrease was noted in the hyalinized collagen bundles at weeks 1 to 4 after treatment, compared with the DMSO control group (Figure 10). In contrast, rapamycin caused minimal changes at day 3 to week 4 when compared with the P529 treatment group.

Because KD exhibits increased ECM formation and blood vessel density[19,23,47] compared with normal dermis (see Supplemental Figure S2 at *http://ajp.amjpathol.org*), we wondered whether P529 would exert any anti-angiogenic effects in an *ex vivo* model of KD. P529 showed a significant reduction in vascular density, as visualized by CD31 and expression of CD34 immunostaining. In addition, CD31+ cell density (endothelial cell marker) (n = 8) (Figure 10B) and expression of CD34+ immunoreactivity (n = 6) (see Supplemental Figure S11 at *http://ajp.amjpathol.org*) were drastically reduced at week 1 after treatment with both P529 and wortmannin compared with rapamycin. Thus, P529 exerts strong anti-inflammatory and anti-angiogenic properties in KD tissue.

P529 Inhibits KD Proliferation and Promotes Its Apoptosis in Situ

From shrinkage of KD volume and epidermal thickness, we hypothesized that P529 may inhibit proliferation and cause apoptosis in the keloid *ex vivo* model. To address this, we further analyzed the effect of P529 on proliferation and induction of apoptosis in keloid OC (n = 6) up to 4 weeks. P529 (20 ng/mL) showed marked reduction in PCNA expression at week 1 compared with vehicle-treated controls (see Supplemental Figure S12 at *http://ajp.amjpathol.org*). Furthermore, P529 significantly ($P <$ 0.05) increased apoptosis at week 1 in keloid OC compared with groups treated with vehicle, rapamycin, and wortmannin (Figure 11, A and B). After 4 weeks, P529

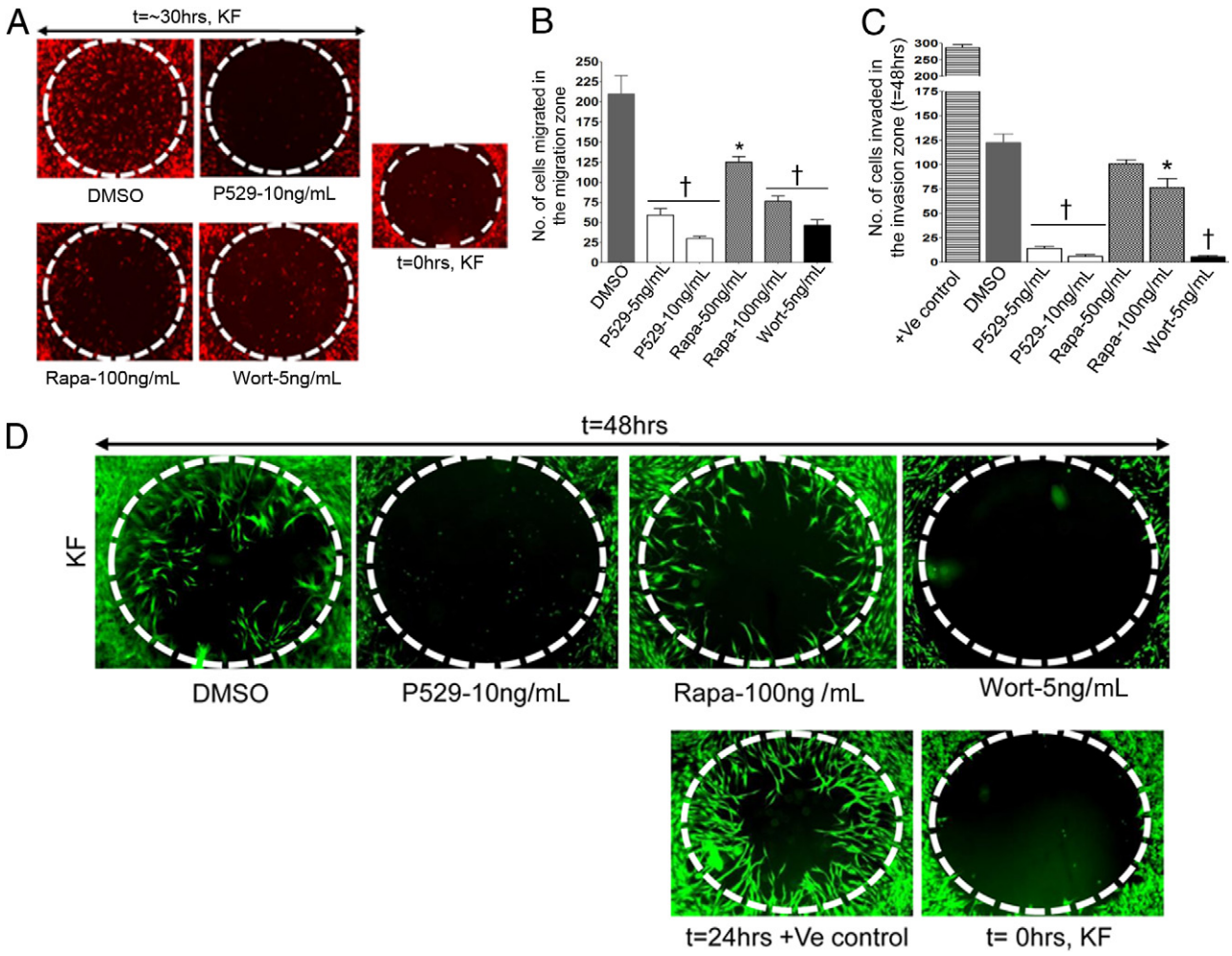

Figure 7. Effect of P529, rapamycin, and wortmannin drugs on KF migration and invasion properties in *in vitro* 2D and 3D models, respectively. **A:** KF migration response toward 2-mm migration zone created by cell seeding stoppers in the presence and absence of various drugs. Representative micrographs are shown from three independent experiments. **B:** Number of migrated KF in the migration zone with and without drugs. Number of cells migrated into the migration zone were counted on the basis of the 0 hour migration pattern and plotted on the graph. **C:** Number of invaded KF in the invasion zone with and without drugs. Number of cells invaded into the invasion zone were counted on the basis of the 0 hour invasion pattern and plotted on the graph. **D:** KF invasive response toward 2-mm invasion zone created by cell seeding stoppers in the presence and absence of various drugs. Representative micrographs are shown from three independent experiments. $^{*}P < 0.05$, $^{\dagger}P < 0.02$, significant difference in drug-treated group vs DMSO control group.

exerted the most significant apoptosis-promoting effect in KD OC.

Early Inhibition of PI3K/Akt/mTOR signaling in an ex Vivo *Keloid Model*

We also assessed the inhibitory effect of P529 compared with rapamycin and wortmannin on intracellular signaling in an *ex vivo* model. Keloid OC ($n = 8$) tissue was assessed via immunohistochemistry for expression of mTOR pathway–related markers after various drug treatments at different times.

In the P529 treatment group, expression of p-Akt-S473, p-mTOR, and p-S6 were already significantly reduced at week 1, compared with the rapamycin or wortmannin treatment groups. In the rapamycin and wortmannin treatment groups, p-Akt-S473, p-mTOR, and p-S6 (see Supplemental Figure S13, A–C, respectively, at *http://ajp.amjpathol.org*) were reduced at week 1 to week 4, compared with the control group. This suggests that the anti-angiogenic effect of P529 in KD OC could be related to inhibition of mTOR pathway signaling.

Significant Suppression of Collagen I and Fibronectin by P529 in an ex Vivo *Keloid OC Model*

We evaluated the inhibitory effect of P529 on ECM-related markers in the keloid OC ($n = 8$) model. As expected, the immunoreactivity of collagen I was reduced significantly at weeks 1 to 4 after treatment with P529 compared with rapamycin and wortmannin (Figure 12A). All three compounds produced a significant reduction in fibronectin immunoreactivity at week 1 after treatment, compared with the control group. However, the inhibitory effect on fibronectin was noticeably higher with P529 than with rapamycin and wortmannin (Figure 12B). Thus, inhibition of the PI3K/Akt/mTOR signaling pathway by dual

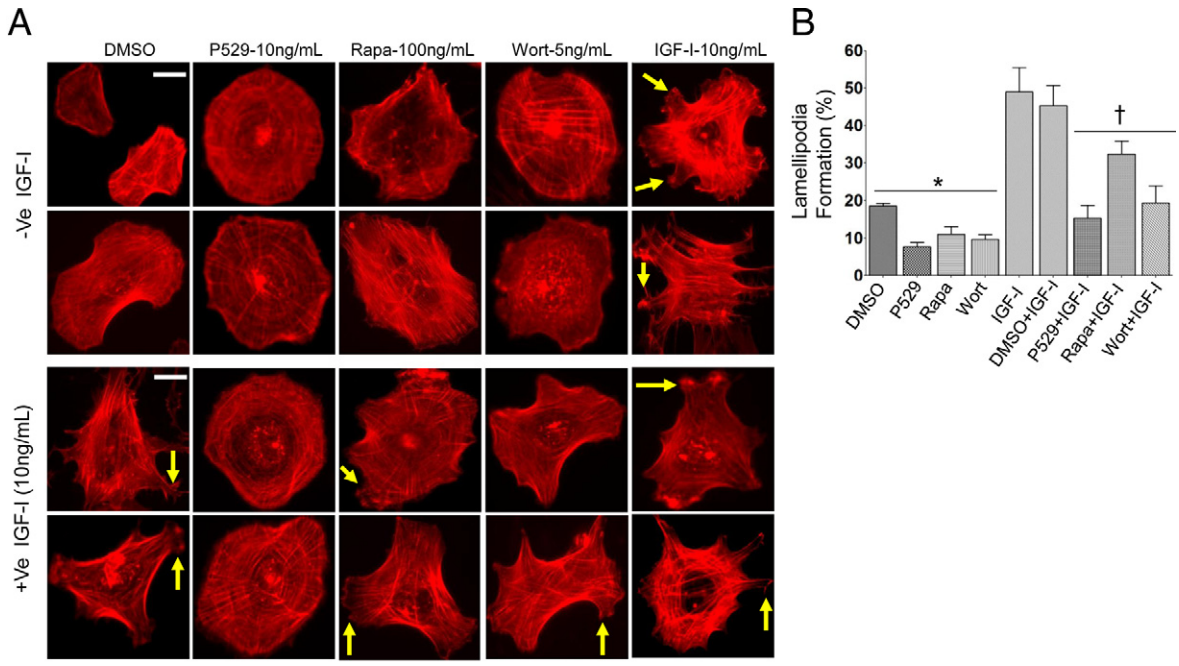

Figure 8. P529 inhibits IGF-I–induced F-actin reorganization. **A:** Representative micrographs from three independent experiments performed in triplicate. In the absence of IGF-I, F-actin was randomly distributed across the cells, as revealed by staining with TRITC-conjugated phalloidin. Some of the F-actin was condensed in dotlike structures at the margins of the cells. However, within 3.5 hours of stimulation with IGF-I, more F-actin was condensed at the leading edge within structures resembling protrusions or lamellipodia-like structures compared with nontreated control cells. Formation of lamellipodia is shown (**arrows**). Scale bar = 20 μm. Micrographs at ×600 magnification. **B:** Percentage of cells with lamellipodia formation. Results are given as mean ± SEM of four independent experiments. $^{*}P < 0.05$, significant difference vs IGF-I group; $^{\dagger}P < 0.05$, significant difference vs DMSO+IGF-I group.

mTORC1 and mTORC2 inhibitor P529 significantly reduced the expression of KD-associated fibrotic markers.

Discussion

Up-regulation of mTOR and its downstream molecules has been well documented in KD.[31–35,48] The present study confirms this by showing overexpression of total mTOR, p70S6K, and their phosphorylated forms and provides the first evidence that p-S6, a key downstream target of mTOR, is also overexpressed in KD. mTOR inhibitors such as rapalogs have been studied in KD previously using *in vitro* primary cell culture models.[31,33,35]Although rapalogs are efficacious in some tumors, their feedback activation may limit their clinical usefulness.[23,25] The dual mTORC1/2 inhibitor P529[24,27,51] exhibits considerably higher anti-KD activity than does the allosteric mTORC1 inhibitor rapamycin,[66] and wortmannin[67,68] a specific covalent inhibitor of PI3K.

The PI3k/Akt/mTOR pathway has proximal and distal feedback signaling, and although mTOR is a downstream effector of Akt, mTORC2 can phosphorylate Akt at a specific site (Ser473), which then hyperactivates Akt via a feedback mechanism.[69] Rapamycin and its analogs (rapalogs) or rapamycin mTOR inhibitors are limited in that they do not affect mTORC2; consequently, duration of inhibition was shortened due to feedback activation of Akt.[70]

Pharmacologic agents such as LY294002 and wortmannin target the P110α catalytic subunit of PI3K.[72] Perifosine and PX-866 are lipid-based Akt inhibitors. Tricirbine (API-2) is selective for Akt-2 inhibition.[71,72] However, targeting proximal pathway components generally results in broad inhibition of the downstream signaling cascade and may augment undesirable effects, whereas P529, a small-molecule synthetic nonsteroidal compound with a chemical structure derived from dibenzo[c]-chromen-6-one, is an allosteric dual mTORC1/2 dissociative inhibitor that abrogates compensatory feedback loop activation. The P529 mechanism of action is unique in that it dissociates the various proteins in the mTORC1/2 complex rather than inhibiting via catalytic competitive inhibition.[27,73]

In the present study, P529 and wortmannin attenuated p-Akt(Ser473), p-mTOR, and ribosomal protein pS6 phosphorylation *in vitro* and *ex vivo*. In contrast, rapamycin failed to inhibit pAkt(Ser473), p-mTOR, and pS6 as potently as did P529. Our P529 findings concur with those of previous studies that showed inhibition of the PI3K/Akt/mTOR axis by this drug.[27,52] Compared with rapamycin, inhibition with both P529 and wortmannin produced a greater reduction in downstream effectors of mTOR in *in vitro* and *ex vivo* models.

Compared with rapamycin, both P529 and wortmannin demonstrated more effective inhibition of cell attachment, spreading, and cell proliferation, caused significant toxicity, and inhibited viability/metabolic activity. Consistent with our results, P529 caused significant cell proliferation, inhibition, and cytotoxicity.[27,51] Treatment with rapamycin[31] and the green tea extract EGCG (epigallocatechin),[32,61] a natural PI3K/Akt/mTOR inhibitor,[49] also showed significant inhibition of primary KF proliferation

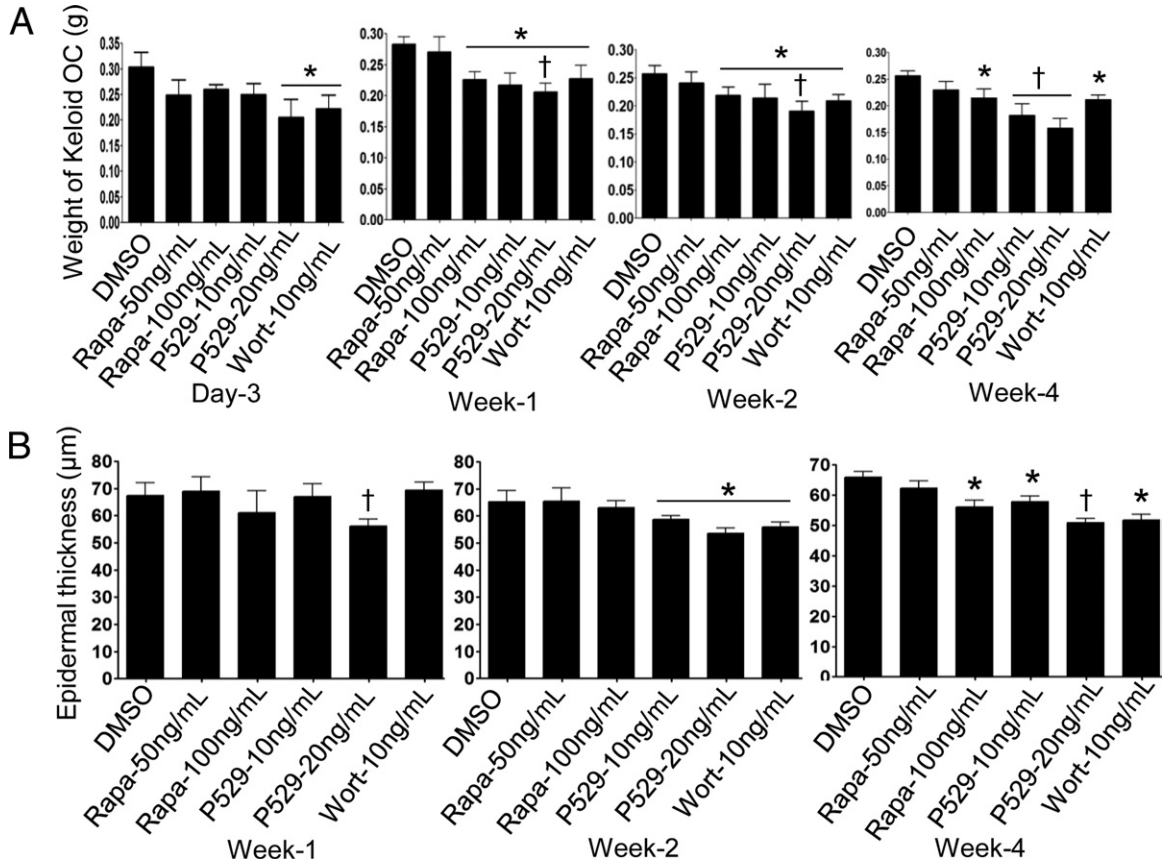

Figure 9. Shrinkage of keloid organ culture (OC) after various drug treatments. Four-millimeter keloid tissue explants were maintained in collagen gel matrix in the presence of various concentrations of drugs up to 4 weeks, and the tissue was collected at different times, as indicated in the bar graphs. **A:** Average weights of the keloid tissue OC at different times are indicated in the bar graph. **B:** Mean length of all layers of epidermal shrinkage except stratum corneum, given in micrometers, shows a significant reduction of epidermal thickness in the treated group vs the untreated control group.*$P < 0.05$, †$P < 0.02$, significant difference vs vehicle control group.

and migration. P529 sustained a significant inhibitory effect on primary KF (5 ng/mL) and NF (20 ng/mL) activity, compared with rapamycin and wortmannin, after discontinuation of the drugs. Primary KF recovered from rapamycin mode of action within 3 days.[31] However, in the present study, all three drugs, P529, rapamycin, and wortmannin, had no reversibility effect after discontinuation of the drug at up to 30 hours. Thus, it seems that

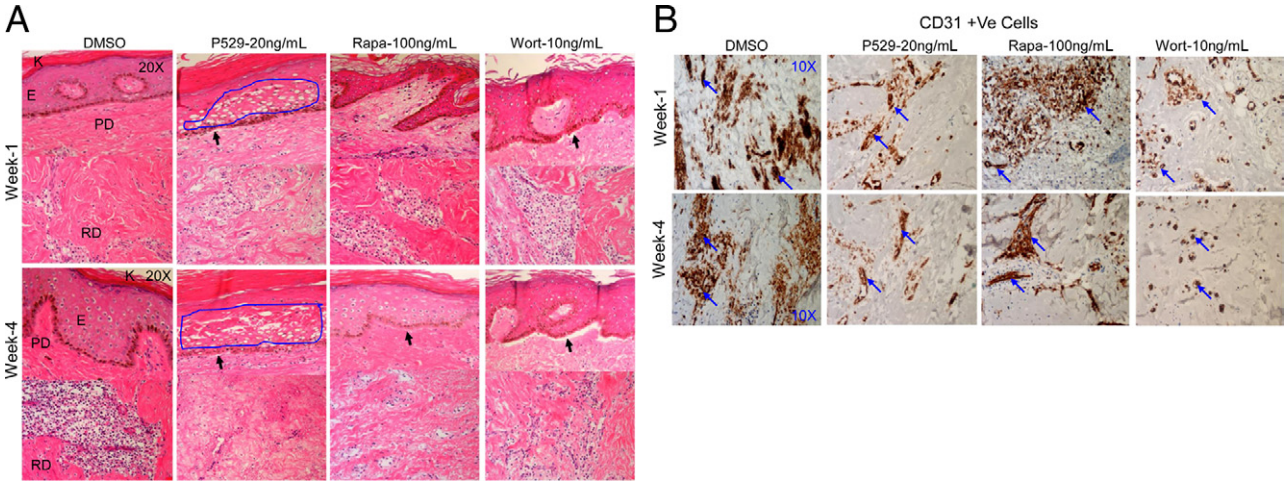

Figure 10. Effect of P529 on keloid OCcellularity/inflammation and angiogenesis. **A:** Morphologic analysis of keloid OC tissue after various drug treatments using H&E staining. Tissue was collected after different drug treatments at various times as indicated. H&E staining of tissue sections was performed using standard protocols. Micrographs were obtained using an Olympus BX21 microscope at ×200 magnification. E, epidermis; K, keratin layer; PD, papillary dermis; RD, reticular dermis. **Arrows** indicate the dislocation of epidermis from dermis after treatment. Pyknotic nuclei are shown in the blue circle. **Arrows** indicate dislocation of epidermis in the treated groups. **B:** Immunoperoxidase analysis of CD31+ endothelial cell marker after various drug treatments in keloid OC model. Original magnification 100. **Arrows** shows the staining pattern for CD31+ cells in the treated and untreated groups.

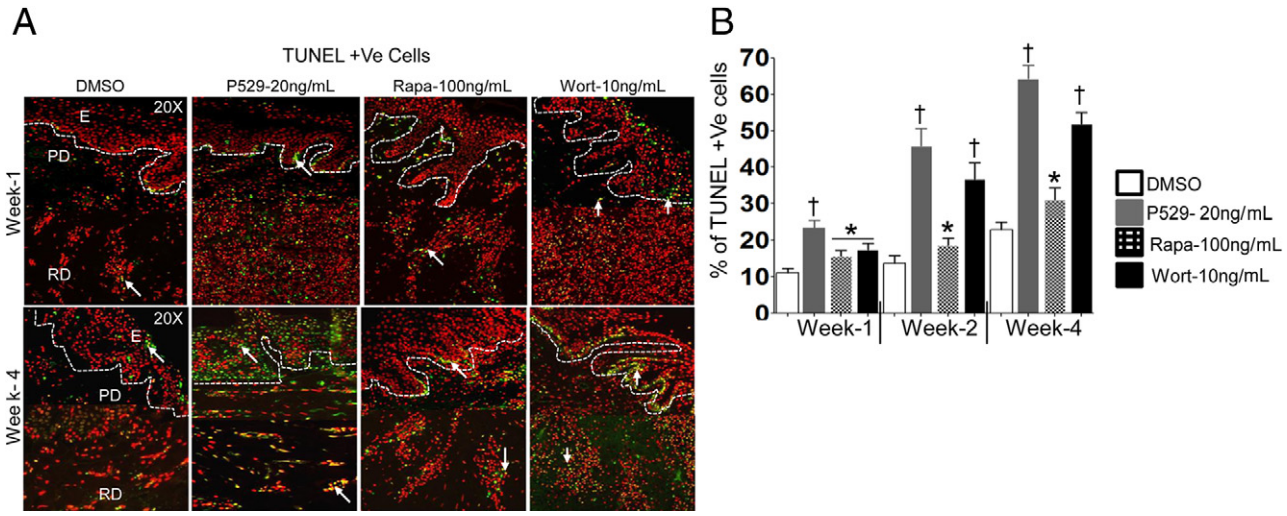

Figure 11. Effect of P529 on keloid cell apoptosis in OC model. Four-millimeter keloid OC was treated with various drug concentrations as indicated. **A:** P529 induces massive apoptosis in keloid OC. TUNEL staining (red nuclei and green-yellow TUNEL-positive cells). The **dotted lines** indicate demarcation of epidermis and dermis junction. Original magnification ×200. E, epidermis; PD, papillary dermis; RD, reticular dermis. **B:** Morphometric analysis of percentage of TUNEL-positive cells. $^{*}P < 0.05$, $^{\dagger}P < 0.02$, significant difference vs DMSO control group. **Arrows** indicate TUNEL-positive cells in the treated and untreated groups.

P529 is selective and more efficacious in inhibiting primary KF.

In 2D and 3D culture models, P529 and wortmannin inhibited migration and invasion properties of KF more effectively than did rapamycin. This might have been achieved by suppressing F-actin, PCNA, and cyclin D. Consistent with our P529 data, recently it has been shown that mTORC2 controls F-actin reorganization,[22,26,28,63] and this F-actin reorganization can be inhibited by dual inhibitors such as P529[24,27] and AZD8055.[6,28,30] Activation of the PI3K/Akt/mTOR pathway is important for cell survival and cell growth.[74] Because inhibition of PI3K/Akt/mTOR induces apoptosis,[24,27,51] we analyzed the effect of P529 on KD apoptosis. Both, P529 and wortmannin produced marked apoptosis *in vitro* and *ex vivo*. In contrast, rapamycin produced minimal apoptosis. Consistent with our results, P529 significantly increased apoptosis in tumor cells.[27,51] In addition, P529 was more potent than wortmannin in inducing apoptosis.

PCNA and cyclin D are downstream molecular markers that can be used to monitor the biological effects of mTOR on fibroblasts.[31] In the present study, P529 strongly inhibited PCNA *in vitro* and *ex vivo* and cyclin D *in vitro*. These data indicated specificity of P529 in KD. Corroborating our findings, Ong et al[31] also found that rapamycin inhibits PCNA and cyclin D in primary KF.

Both P529 and wortmannin, compared with rapamycin, demonstrated reduced cellularity, inflammation, and hyalinized collagen bundles. We further explored the efficacy of P529 by assessing shrinkage of keloid OC tissue volume and epidermal thickness. These findings demonstrated that shrinkage of keloid OC resulted in reduction of average keloid OC volume and significant shrinkage of

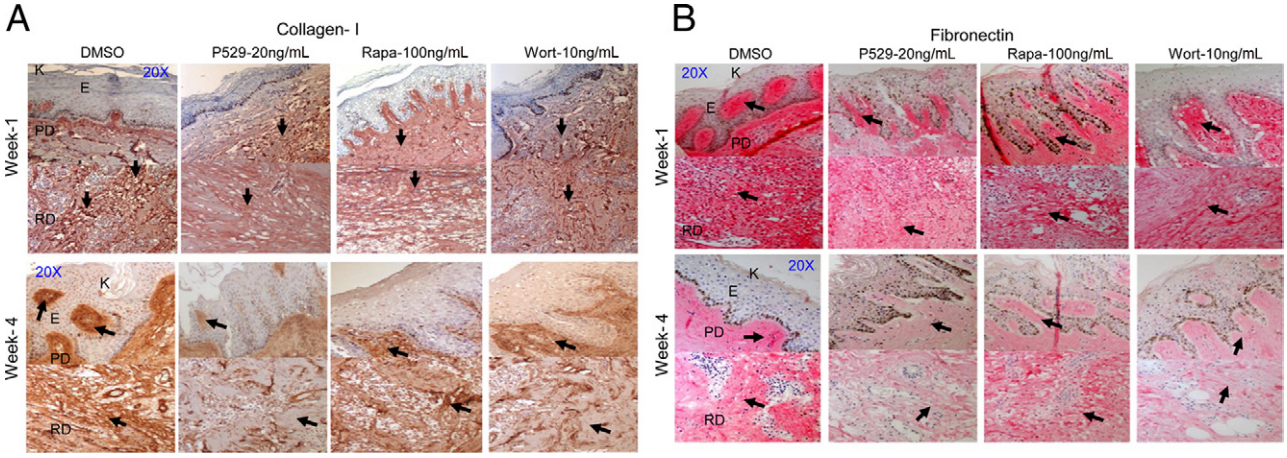

Figure 12. Effect of P529 on collagen and fibronectin biosynthesis in the keloid OC model. **A:** Reduction of collagen I biosynthesis expression by P529 treatment in keloid OC model. **B:** Inhibition of fibronectin expression by P529 treatment in keloid OC model. Original magnification ×200. E, epidermis; K, keratin layer; PD, papillary dermis; RD, reticular dermis. **Arrows,** intensity of staining with and without treatment.

OC epidermis at week 1 after treatment with both P529 and wortmannin at very low concentrations (20 and 10 ng/mL, respectively), compared with rapamycin (100 ng/mL). This could be achieved by inhibition of PCNA and significant induction of apoptosis. Consistent with our results, in other tumors, P529 considerably reduced tumor growth and volume,[24,27,51] and treatment with EGCG reduced KF nodules *in vivo*.[32] Compared with rapamycin, the effect of both P529 and wortmannin on angiogenesis showed significant reduction in CD31+ cells and expression of CD34+ immunoreactivity. Rapamycin did inhibit CD31+ cells at a much higher concentration (100 ng/mL) than did P529 and wortmannin at weeks 1 to 4. Supporting our findings in keloid OC, P529 reduces CD31+ cells in other tumors.[27]

Akt is a central element in the PI3K/Akt/mTOR network, and there is increasing evidence that this pathway has an important role in KD pathogenesis.[31,32,34,35] The role of PI3K in collagen regulation has been demonstrated in human dermal fibroblasts.[75,76] In addition, multiple downstream targets of PI3K, including Akt and mTOR, have been linked to collagen regulation.[31,45,46,77] Recently, it was demonstrated that the PI3K/Akt/mTOR axis may have a pivotal role in fibronectin transcription.[31,78] Rapamycin reduced glomerular α-SMA overexpression.[79] In addition, rapamycin-treated rats with ligated bile ducts have lower volume fractions of connective tissue and cells positive for α-SMA.[80] Collagen, fibronectin, and α-SMA are proteins considered characteristic of the keloid tissue phenotype.[66] Compared with rapamycin, both P529 and wortmannin more significantly reduced the keloid-associated fibrotic markers collagen I, fibronectin, and α-SMA in our *in vitro* model, and collagen I and fibronectin in our *ex vivo* model. Furthermore, the overall inhibitory effect on expression levels of collagen, fibronectin, and α-SMA were higher with P529 than with rapamycin and wortmannin. In line with our results, Ong et al[31] also found that treatment of mTOR inhibitor (rapamycin) significantly reduced ECM and α-SMA in primary KF.

P529 is highly effective in KF compared with NF, even at low concentrations, which suggests that P529 is a highly selective inhibitor of mTOR. This could be due to a more active PI3K/Akt/mTOR axis in keloids compared with normal skin. It is unlikely that complete target inhibition could be sustained over long periods in patients with KD because PI3K signaling is critical in the maintenance of normal tissue, although, it is possible that higher doses given intermittently and intralesionally might result in a better therapeutic outcome by producing sustained PI3K/Akt/mTOR inhibition in KD, while allowing time for normal tissue recovery. An alternative strategy would be to combine PI3K/Akt/mTOR inhibitors with anti-cancer agents that target other signaling pathways, which are considered to be dysregulated in KD.

Clinically adverse events have been associated with the use of the mTORC1 inhibitor rapamycin and its analogs.[73] However, with P529, such toxicities have not been observed to date in ongoing human phase I trials. P529 showed no toxicity in toxicology studies in dogs and rats. It is important to note that no *in vivo* toxicity was observed when P529 was administered in dose-ranging studies in dogs and rabbits.[81] However, it remains to be formally concluded that P529 may not only inhibit keloid growth but also normal wound healing.[27,74,81]

In conclusion, the present study provides the first available functional evidence that the PI3K/Akt/mTOR axis is an important target in KD treatment *in situ*. Moreover, we show that dual inhibition of the PI3K/Akt/mTOR kinases by P529 can inhibit cell proliferation, migration, cellular invasion, inflammation, and ECM production; reduce tissue volume (shrinkage) and epidermal thickness; and induce apoptosis. Thus, this dual mTOR inhibitor deserves to be systemically explored as an attractive therapeutic option in the future treatment of KD.

Acknowledgments

We thank the GAT Family Foundation for support of this work and sponsoring the collaboration that took place between Prof. Pandolfi and Dr. Bayat's group and the study participants and nursing staff of the University Hospital of South Manchester NHS Foundation Trust (Manchester, UK).

References

1. Watanabe R, Wei L, Huang J: mTOR signaling. function, novel inhibitors, and therapeutic targets. J Nucl Med 2011, 52:497–500
2. Garcia-Echeverria C: Blocking the mTOR pathway: a drug discovery perspective. Biochem Soc Trans 2011, 39:451–455
3. Fasolo A, Sessa C: Current and future directions in mammalian target of rapamycin inhibitors development. Exp Opin Invest Drugs 2011, 20:381–394
4. Ahn JH, Ahn SK, Lee M: The role of autophagy in cytotoxicity induced by new oncogenic B-Raf inhibitor UI-152 in v-Ha-ras transformed fibroblasts. Biochem Biophys Res Commun 2011, 417:857–863
5. Guertin DA, Sabatini DM: Defining the role of mTOR in cancer. Cancer Cell 2007, 12:9–22
6. Sini P, James D, Chresta C, Guichard S: Simultaneous inhibition of mTORC1 and mTORC2 by mTOR kinase inhibitor AZD8055 induces autophagy and cell death in cancer cells. Autophagy 2010, 6:553–554
7. Liu Q, Thoreen C, Wang J, Sabatini D, Gray NS: mTOR mediated anti-cancer drug discovery. Drug Discov Today Ther Strateg 2009, 6:47–55
8. Dazert E, Hall MN: mTOR signaling in disease. Curr Opin Cell Biol 2011, 23:744–755
9. Strimpakos AS, Karapanagiotou EM, Saif MW, Syrigos KN: The role of mTOR in the management of solid tumors: an overview. Cancer Treatment Rev 2009, 35:148–159
10. Nakashima M, Chung S, Takahashi A, Kamatani N, Kawaguchi T, Tsunoda T, Hosono N, Kubo M, Nakamura Y, Zembutsu H: A genome-wide association study identifies four susceptibility loci for keloid in the Japanese population. Nat Genetics 2010, 42:768–771
11. Marneros AG, Norris JEC, Watanabe S, Reichenberger E, Olsen BR: Genome scans provide evidence for keloid susceptibility loci on chromosomes 2q23 and 7p11. J Invest Dermatol 2004, 122:1126–1132
12. Mall JW, Pollmann C, Müller JM, Büttemeyer R: Keloid of the earlobe after ear piercing: not only a surgical problem [in German]. Chirurg 2002, 73:514–516
13. Vincent AS, Phan TT, Mukhopadhyay A, Lim HY, Halliwell B, Wong KP: Human skin keloid fibroblasts display bioenergetics of cancer cells. J Invest Dermatol 2007, 128:702–709
14. Yoshimoto H, Ishihara H, Ohtsuru A, Akino K, Murakami R, Kuroda H, Namba H, Ito M, Fujii T, Yamashita S: Overexpression of insulin-like

growth factor-1 (IGF-I) receptor and the invasiveness of cultured keloid fibroblasts. Am J Pathol 1999, 154:883–889
15. Jiang DY, Fu XB, Chen W, Sun TZ: [Relationship of overexpression of angiogenesis factors and their receptors with invasive growth of keloid]. Chinese. Chin J Plast Surg 2004, 20:128–131
16. Ohtsuru A, Yoshimoto H, Ishihara H, Namba H, Yamashita S: Insulin-like growth factor-I (IGF-I)/IGF-I receptor axis and increased invasion activity of fibroblasts in keloid. Endocr J 2000, 47(Suppl):S41–S44
17. Wu WS, Wang FS, Yang KD, Huang CC, Kuo YR: Dexamethasone induction of keloid regression through effective suppression of VEGF expression and keloid fibroblast proliferation. J Invest Dermatol 2006, 126:1264–1271
18. Wu Y, Zhang Q, Ann DK, Akhondzadeh A, Duong HS, Messadi DV, Le AD: Increased vascular endothelial growth factor may account for elevated level of plasminogen activator inhibitor-1 via activating ERK1/2 in keloid fibroblasts. Am J Physiol Cell Physiol 2004, 286: C905–C912
19. Syed F, Bayat A: Notch signaling pathway in keloid disease: enhanced fibroblast activity in a Jagged-1 peptide dependent manner in lesional versus extra-lesional fibroblasts. Wound Repair Regeneration 2012, 20:688–706
20. Boyce DE, Ciampolini J, Ruge F, Harding KG, Murison MMSC: Inflammatory cell subpopulations in keloid scars. Br J Plast Surg 2001, 54:511–516
21. Shaker SA, Ayuob NN, Hajrah NH: Cell talk: a phenomenon observed in the keloid scar by immunohistochemical study. Appl Immunohistochem Mol Morphol 2011, 19:153
22. Bracho-Valdes I, Moreno-Alvarez P, Valencia-Martienz I, Robles-Molina E, Chavez-Vargas L, Vazquez-Prado J: mTORC1 and mTORC2-interacting proteins keep their multifunctional partners focused. IUBMB Life 2011, 63:896–914
23. Benjamin D, Colombi M, Moroni C, Hall MN: Rapamycin passes the torch: a new generation of mTOR inhibitors. Nat Rev Drug Discovery 2011, 10:868–880
24. Gravina GL, Marampon F, Petini F, Biordi L, Sherris D, Jannini EA, Tombolini V, Festuccia C: The TORC1/TORC2 inhibitor, Palomid 529, reduces tumor growth and sensitizes to docetaxel and cisplatin in aggressive and hormone-refractory prostate cancer cells. Endocr Relat Cancer 2011, 18:385–400
25. Yu K, Shi C, Toral-Barza L, Lucas J, Shor B, Kim JE, Zhang WG, Mahoney R, Gaydos C, Tardio LA: Beyond rapalog therapy: preclinical pharmacology and antitumor activity of WYE-125132, an ATP-competitive and specific inhibitor of mTORC1 and mTORC2. Cancer Res 2010, 70:621–631
26. Sparks CA, Guertin DA: Targeting mTOR: prospects for mTOR complex 2 inhibitors in cancer therapy. Oncogene 2010, 29:3733–3744
27. Xue Q, Hopkins B, Perruzzi C, Udayakumar D, Sherris D, Benjamin LE: Palomid 529, a novel small-molecule drug, is a TORC1/TORC2 inhibitor that reduces tumor growth, tumor angiogenesis, and vascular permeability. Cancer Res 2008, 68:9551–9557
28. Chresta CM, Davies BR, Hickson I, Harding T, Cosulich S, Critchlow SE, Vincent JP, Ellston R, Jones D, Sini P: AZD8055 is a potent, selective, and orally bioavailable ATP-competitive mammalian target of rapamycin kinase inhibitor with in vitro and in vivo antitumor activity. Cancer Res 2010, 70:288–298
29. Garcia-Martinez JM, Moran J, Clarke RG, Gray A, Cosulich SC, Chresta CM, Alessi DR: Ku-0063794 is a specific inhibitor of the mammalian target of rapamycin (mTOR). Biochem J 2009, 421: 29–42
30. Marshall G, Howard Z, Dry J, Fenton S, Heathcote D, Gray N, Keen H, Logie A, Holt S, Smith P: Benefits of mTOR kinase targeting in oncology: pre-clinical evidence with AZD8055. Biochem Soc Trans 2011, 39:456–459
31. Ong CT, Khoo YT, Mukhopadhyay A, Do DV, Lim IJ, Aalami O, Phan TT: mTOR as a potential therapeutic target for treatment of keloids and excessive scars. Exp Derm 2007, 16:394–404
32. Zhang Q, Kelly AP, Wang L, French SW, Tang X, Duong HS, Messadi DV, Le AD: Green tea extract and (-)-epigallocatechin-3-gallate inhibit mast cell-stimulated type I collagen expression in keloid fibroblasts via blocking PI-3K/Akt signaling pathways. J Invest Dermatol 2006, 126:2607–2613
33. Khoo YT, Ong CT, Mukhopadhyay A, Han HC, Do DV, Lim IJ, Phan TT: Upregulation of secretory connective tissue growth factor (CTGF) in keratinocytes-fibroblast coculture contributes to keloid pathogenesis. J Cell Physiol 2006, 208:336–343
34. Mukhopadhyay A, Do DV, Ong CT, Khoo YT, Masilamani J, Chan SY, Vincent AS, Wong PK, Lim CP, Cao X: The role of SCF and c-KIT in keloid pathogenesis: do tyrosine kinase inhibitors have a potential therapeutic role? Br J Dermatol 2010, 164:372–386
35. Do DV, Ong CT, Khoo YT, Carbone A, Lim CP, Wang S, Mukhopadhyay A, Cao X, Cho DH, Wei XQ: Interleukin-18 system plays an important role in keloid pathogenesis via epithelial-mesenchymal interactions. Br J Dermatol 2012, 166:1275–1288
36. Bagabir R, Syed F, Paus R, Bayat A: Long-term organ culture of keloid disease tissue. Exp Dermatol 2012, 21:376–381
37. Shih B, Garside E, McGrouther DA, Bayat A: Molecular dissection of abnormal wound healing processes resulting in keloid disease. Wound Repair Regen 2010, 18:139–153
38. Mall JW, Pollmann C, Muller JM, Buttemeyer R: [Keloid of the earlobe after ear piercing: not only a surgical problem]. German. Chirurg 2002, 73:514–516
39. Mukhopadhyay A, Do DV, Ong CT, Khoo YT, Masilamani J, Chan SY, Vincent AS, Wong PK, Lim CP, Cao X: The role of SCF and c-KIT in keloid pathogenesis: do tyrosine kinase inhibitors have a potential therapeutic role? Br J Dermatol 2011, 164:372–386
40. Anthony ET, Lemonas P, Navsaria HA, Moir GC: The cost effectiveness of intralesional steroid therapy for keloids. Dermatol Surg 2010, 36:1624–1626
41. Bermueller C, Rettinger G, Keck T: Auricular keloids: treatment and results. Eur Arch Otorhinolaryngol 2010, 267:575–580
42. Patel NP, Lawrence Cervino A: Keloid treatment: is there a role for acellular human dermis (Alloderm)? J Plast Reconstr Aesthet Surg 2010, 63:1344–1348
43. Larios G, Gregoriou S, Rigopoulos D: Letter: further options for treatment of hypertrophic scars and keloids. Dermatol Surg 2010, 36:268–269
44. Juckett G, Hartman-Adams H: Management of keloids and hypertrophic scars. Am Fam Physician 2009, 80:253–260
45. Shegogue D, Trojanowska M: Mammalian target of rapamycin positively regulates collagen type I production via a phosphatidylinositol 3-kinase-independent pathway. J Biol Chem 2004, 279:23166–23175
46. Bujor AM, Pannu J, Bu S, Smith EA, Muise-Helmericks RC, Trojanowska M: Akt blockade downregulates collagen and upregulates MMP1 in human dermal fibroblasts. J Invest Dermatol 2008, 128: 1906–1914
47. Liu HW, Cheng B, Yu WL, Sun RX, Zeng D, Wang J, Liao YX, Fu XB: Angiotensin II regulates phosphoinositide 3 kinase/Akt cascade via a negative crosstalk between AT1 and AT2 receptors in skin fibroblasts of human hypertrophic scars. Life Sci 2006, 79:475–483
48. Liao WT, Yu HS, Arbiser JL, Hong CH, Govindarajan B, Chai CY, Shan WJ, Lin YF, Chen GS, Lee CH: Enhanced MCP-1 release by keloid CD14+ cells augments fibroblast proliferation: role of MCP-1 and Akt pathway in keloids. Exp Dermatol 2010, 19:e142–e150
49. Zhou H, Luo Y, Huang S: Updates of mTOR inhibitors. Anticancer Agents Med Chem 2010, 10:571–581
50. Lin F, Sherris D, Beijnen JH, Van Tellingen O: High-performance liquid chromatography analysis of a novel small-molecule, anti-cancer drug, Palomid 529, in human and mouse plasma and in mouse tissue homogenates. J Chromatogr B Analyt Technol Biomed Life Sci 2011, 879:3823–3831
51. Diaz R, Nguewa PA, Diaz-Gonzalez JA, Hamel E, Gonzalez-Moreno O, Catena R, Serrano D, Redrado M, Sherris D, Calvo A: The novel Akt inhibitor Palomid 529 (P529) enhances the effect of radiotherapy in prostate cancer. Br J Cancer 2009, 100:932–940
52. Xiang T, Jia Y, Sherris D, Li S, Wang H, Lu D, Yang Q: Targeting the Akt/mTOR pathway in Brca1-deficient cancers. Oncogene 2011, 30: 2443–2450
53. Hsieh AC, Ruggero D: Targeting eukaryotic translation initiation factor 4E (eIF4E) in cancer. Clin Cancer Res 2010, 16:4914–4920
54. Syed F, Ahmadi E, Iqbal SA, Singh S, McGrouther DA, Bayat A: Fibroblasts from the growing margin of keloid scars produce higher levels of collagen I and III compared with intralesional and extralesional sites: clinical implications for lesional site-directed therapy. Br J Dermatol 2011, 164:83–96
55. Syed F, Thomas A, Singh S, Kolluru V, Emeigh Hart S, Bayat A: In vitro study of novel collagenase (Xiaflex) on Dupuytren's disease fibro-

blasts displays unique drug related properties. PloS One 2012, 7:e31430
56. Atienza JM, Zhu J, Wang X, Xu X, Abassi Y: Dynamic monitoring of cell adhesion and spreading on microelectronic sensor arrays. J Biomol Screening 2005, 10:795–805
57. Lu Z, Hasse S, Bodo E, Rose C, Funk W, Paus R: Towards the development of a simplified long-term organ culture method for human scalp skin and its appendages under serum-free conditions. Exp Dermatol 2007, 16:37–44
58. Ma XM, Blenis J: Molecular mechanisms of mTOR-mediated translational control. Nat Rev Mol Cell Biol 2009, 10:307–318
59. Hay N, Sonenberg N: Upstream and downstream of mTOR. Genes Dev 2004, 18:1926–1945
60. Calderon M, Lawrence WT, Banes AJ: Increased proliferation in keloid fibroblasts wounded in vitro. J Surg Res 1996, 61:343–347
61. Park G, Yoon BS, Moon JH, Kim B, Jun EK, Oh S, Kim H, Song HJ, Noh JY, Oh CH: Green tea polyphenol epigallocatechin-3-gallate suppresses collagen production and proliferation in keloid fibroblasts via inhibition of the STAT3-signaling pathway. J Invest Dermatol 2008, 128:2429–2441
62. Ridley AJ, Schwartz MA, Burridge K, Firtel RA, Ginsberg MH, Borisy G, Parsons JT, Horwitz AR: Cell migration: integrating signals from front to back. Science 2003, 302:1704–1709
63. Jacinto E, Loewith R, Schmidt A, Lin S, Ruegg MA, Hall A, Hall MN: Mammalian TOR complex 2 controls the actin cytoskeleton and is rapamycin insensitive. Nat Cell Biol 2004, 6:1122–1128
64. Liu L, Chen L, Chung J, Huang S: Rapamycin inhibits F-actin reorganization and phosphorylation of focal adhesion proteins. Oncogene 2008, 27:4998–5010
65. Hsu YC, Chen MJ, Yu YM, Ko SY, Chang CC: Suppression of TGF-β1/SMAD pathway and extracellular matrix production in primary keloid fibroblasts by curcuminoids: its potential therapeutic use in the chemoprevention of keloid. Arch Dermatol Res 2010, 302:1–8
66. Roychowdhury A, Sharma R, Kumar S: Recent advances in the discovery of small molecule mTOR inhibitors. Future 2010, 2:1577–1589
67. Yuan TL, Cantley LC: PI3K pathway alterations in cancer: variations on a theme. Oncogene 2008, 27:5497–5510
68. Knight ZA, Shokat KM: Chemically targeting the PI3K family. Biochem Soc Trans 2007, 35:245–249
69. Bhagwat SV, Crew AP: Novel inhibitors of mTORC1 and mTORC2. Curr Opin Invest Drugs 2010, 11:638–645
70. Yip CK, Murata K, Walz T, Sabatini DM, Kang SA: Structure of the human mTOR complex I and its implications for rapamycin inhibition. Mol Cell 2010, 38:768–774
71. Bain J, Plater L, Elliott M, Shpiro N, Hastie CJ, McLauchlan H, Klevernic I, Arthur JSC, Alessi DR, Cohen P: The selectivity of protein kinase inhibitors: a further update. Biochem J 2007, 408:297–315
72. LoPiccolo J, Blumenthal GM, Bernstein WB, Dennis PA: Targeting the PI3K/Akt/mTOR pathway: effective combinations and clinical considerations. Drug Resist Updates 2008, 11:32–50
73. Lewis GP, Chapin EA, Byun J, Luna G, Sherris D, Fisher SK: Muller cell reactivity and photoreceptor cell death are reduced after experimental retinal detachment using an inhibitor of the Akt/mTOR pathway. Invest Ophthalmol Vis Sci 2009, 50:4429–4435
74. Morgensztern D, McLeod HL: PI3K/Akt/mTOR pathway as a target for cancer therapy. Anticancer Drugs 2005, 16:797–803
75. Jinnin M, Ihn H, Yamane K, Tamaki K: Interleukin-13 stimulates the transcription of the human alpha 2 (I) collagen gene in human dermal fibroblasts. J Biol Chem 2004, 279:41783–41791
76. Asano Y, Ihn H, Yamane K, Jinnin M, Mimura Y, Tamaki K: Phosphatidylinositol 3-kinase is involved in alpha 2(I) collagen gene expression in normal and scleroderma fibroblasts. Journal Immunol 2004, 172:7123–7135
77. Svegliati Baroni G, Ridolfi F, Di Sario A, Saccomanno S, Bendia E, Benedetti A, Greenwel P: Intracellular signaling pathways involved in acetaldehyde-induced collagen and fibronectin gene expression in human hepatic stellate cells. Hepatology 2001, 33:1130–1140
78. White ES, Sagana RL, Booth AJ, Yan M, Cornett AM, Bloomheart CA, Tsui JL, Wilke CA, Moore BB, Ritzenthaler JD: Control of fibroblast fibronectin expression and alternative splicing via the PI3K/Akt/mTOR pathway. Exp Cell Res 2010, 316:2644–2653
79. Lloberas N, Cruzado JM, Franquesa M, Herrero-Fresneda I, Torras J, Alperovich G, Rama I, Vidal A, Grinyó JM: Mammalian target of rapamycin pathway blockade slows progression of diabetic kidney disease in rats. J Am Soc Nephrol 2006, 17:1395–1404
80. Biecker E, De Gottardi A, Neef M, Unternahrer M, Schneider V, Ledermann M, Sagesser H, Shaw S, Reichen J: Long-term treatment of bile duct-ligated rats with rapamycin (sirolimus) significantly attenuates liver fibrosis: analysis of the underlying mechanisms. J Pharmacol Exp Ther 2005, 313:952–961
81. Jacot JL, Sherris D: Potential therapeutic roles for inhibition of the PI3K/Akt/mTOR pathway in the pathophysiology of diabetic retinopathy. J Ophthalmol 2011, 2011:589813